EVALUATION OF RESISTIVITY IMAGING (RI) METHOD FOR DETERMINING UNKNOWN DEEP FOUNDATION DEPTH

by

MOHAMMAD SADIK KHAN

Presented to the Faculty of the Graduate School of

The University of Texas at Arlington in Partial Fulfillment

of the Requirements

for the Degree of

MASTER OF SCIENCE IN CIVIL ENGINEERING

THE UNIVERSITY OF TEXAS AT ARLINGTON

August 2011

ACKNOWLEDGEMENTS

First, I would like to express my deepest gratitude to my supervisor Dr. Sahadat Hossain, for his valuable time, guidance, encouragement, help and unconditional support throughout my Master's studies. Without his constant guidance and support, this thesis would not have been completed.

I would like to give my special thanks to Dr. Mohammad Najafi and Dr. Stefan A. Romanoschi, for their time and participation as my committee members and for their valuable suggestions and advice.

Special thanks extended to Jubair Hossain, Tashfeena Taufiq, Shahed Rezwan Manzur, Golam Kibria, and Sonia Samir for their active cooperation and assistance in all stages of work.

I would also like to thank my dearest friends for their worthy friendship and the good times.

I wish to acknowledge the cooperation, sacrifice and unconditional support from my wife Nusrat Kabir throughout my graduate studies. I would like to thank my sister Sifat Khanm and brother Sadat Khan for giving me support.

Finally, and most of all, I would like to thank my parents for all their love, encouragement, and great support. It is the best thing in my life to be a part of their family

June 30, 2011

ABSTRACT

EVALUATION OF RESISTIVITY IMAGING (RI) METHOD FOR DETERMINING UNKNOWN DEEP FOUNDATION DEPTH

Mohammad Sadik Khan, M.S.

The University of Texas at Arlington, 2011

Supervising Professor: MD. Sahadat Hossain

There are approximately 580,000 highway bridges in the National Bridge inventory and 104,000 of these bridges are estimated to have unknown foundations type and/or depth. Determining unknown foundation length and type of bridge foundation is becoming an important issue for State DOTs to ensure the safety of the bridge. There are several methods available to determine unknown foundation depth based on specific site conditions and type of foundation to be tested. Resistivity Imaging (RI) is a non destructive method to investigate the subsurface condition. The objective of current study was to determine unknown bridge foundation depth of three bridges at North Texas using RI method. Two of the investigated bridges were supported by driven steel H-pile and the other bridge had drill shaft as foundation. Based on RI results, unknown foundation depth were determined from the variation of resistivity below the foundation. Parallel Seismic (PS) and Sonic Echo (SE) method were also utilized for one bridge site supported by steel H pile to verify the depth determined by RI method. PS method was performed in two casing backfilled with sand and cement grout. The investigated unknown bridge foundation depths using RI method were compared with the actual foundation depth. The

determined unknown foundation depths from RI method were found very close to actual foundation depth for two steel H-pile sites. However, no significant variation of resistivity was observed below the foundation of third bridge supported by drill shaft and the determined foundation depth for third bridge site did not match the actual foundation depth. PS method also predicted the depth of the foundation very close to actual foundation depth. However, the SE test was determined to be not suitable for determining the unknown steel H-pile foundation depth.

TABLE OF CONTENTS

LIST OF ILLUSTRATIONS

LIST OF TABLES

CHAPTER 1

INTRODUCTION

1.1 Background

There are approximately 580,000 highway bridges in the National Bridge inventory and 104,000 of these bridges are estimated to have unknown foundations type and/or depth (Olson et al., 1998). Determination of unknown foundation length and type of bridge foundation is becoming an important issue for the State Department of Transportation (DOT) to ensure the safety of the bridge structure. Evaluation of existing foundation differs from the usual Non-Destructive testing (NDT) method in which structure cover the top of deep foundation (Gassman and Finno, 1999). There are several methods for the evaluation (to determine) of unknown foundation depth. The selection of NDT method is dependent on its specific utility and the type of the foundation to be tested.

Several studies have been conducted on the Non Destructive Testing (NDT) method to determine the unknown foundation depth and type. Olson et al. (1998) studied the effectiveness of different Non Destructive Testing (NDT) methods. From the study, several NDT methods are well proved to determine the unknown foundation including the Parallel Seismic method, Sonic Echo (SE) /Impulse Response (IR) method, Dispersion of Bending wave Energy, Ultraseismic methods, Ground Penetrating Radar (GPR), Induction Electromagnetic Field method with borehole. Mercado and O'Neill (2000) performed seismic techniques includes Seismic Wave Reflection Survey (SWRS), Transient forced vibration survey (TFVS) and Parallel Seismic method to determine the pile depth in Houston, Texas. Yu et al., (2007) performed study on different geophysical methods including Impact Echo method; Parallel Seismic method and

Magnetometer method to determine augur cast pile length in sandy soil in Georgia. Stegman and Holt (2000) utilized GPR and Dispersive wave technology to evaluate the capacity of a 100 years old bridge foundation. However, GPR requires site access and access to the exposed top surface of the foundation. In addition, some methods are invasive that required installation of boreholes which may be expensive.

Geophysical methods have the possibility to give an “image” of the subsurface. With the development of new software for the interpretation of resistivity measurements, 2D and 3D “resistivity imaging” or “resistivity tomography” is extensively used now a days in shallow geophysical investigation and geohazard study. Olson et al. (1999) emphasized the possibility and advantage of monitoring resistivity variation in subsurface exploration. Resistivity imaging can be easily carried out over several meters and can be applied to describe both horizontal and vertical variability of soil structure and properties (Tabbagh et al., 2000).

Ground Penetration Radar (GPR) and High Resolution Resistivity (HRR) are commonly used non invasive geophysical method. GPR is a powerful tool to find ground water level, distinguish different layers in subsurface, rupture and cavity. GPR is also utilized to investigate the unknown foundation depth and type of the foundation. GPR uses high frequency electromagnetic wave. The frequency range of GPR is 10 to 1200 MHz which gives a resolution between 0.1m to 3 m. Higher frequency results higher resolution with lower penetration depth. The penetration depth usually ranged from 40-60 m and can reach 300 m in some special cases like unweathered granite or ice. The radar signal affected by dielectric permittivity and electrical conductivity. With higher electrical conductivity in clay soil, deeper radar signal penetration becomes difficult. Therefore, presence of clayed soil in DFW area makes it difficult to interpret GPR data. On the other hand, electrical resistivity imaging can provide subsurface resistivity information both is sandy and clayed soil.

Multichannel electrical resistivity investigations become a popular geophysical exploration technique due to its simple physical principle and efficient data acquisition. In the last decade, there has been great advancement in computerized data acquisition systems and 2D and 3D inversion software. Traditional resistivity measurements are carried out on earth's surface with a specified array in order to obtain apparent resistivity sounding curves, apparent resistivity profiling or apparent resistivity pseudo-sections. The resistivity profile qualitatively reflects vertical or horizontal variations in subsurface resistivity. Due to existence of foundation structure, there will be discontinuity of soil materials and maybe there will be presence of a disturbed soil zone. This disturbance may cause some variation in the resistivity imaging. Thus the disturbed zone below the foundation may be determined by resistivity imaging which can be utilized as a technique to determine the unknown foundation depth.

1.2 Problem Statement

Unknown bridge foundation depth is an important issue to the bridge owner for the bridge safety evaluation. At present, different NDT methods are utilized to a large extent to investigate the foundation type and depth. These existing NDT methods are suitable for specific bridge types, depth of the foundation, site accessibility and subsurface conditions. However, most of the existing NDT methods are invasive and some methods require additional boring to perform the test.

In this study, 2D Electrical Resistivity Imaging was utilized to investigate unknown foundation depth at 3 different bridges located in North Texas region. Two of the bridges have steel H-pile as foundation and the other bridge was supported by Drill Shaft. The foundation depths determined from 2D resistivity imaging are compared to the actual foundation depth.

1.3 Objectives

The objective of the current research was to investigate the effectiveness of Resistivity Imaging (RI) technique to determine unknown bridge foundation depth. Also foundation depths

determined from RI was compared with foundation depths determined using Parallel Seismic (PS) method and Sonic Echo (SE) method. Three different bridge foundations were investigated for the purpose of this study. Resistivity Imaging (RI) was used for determining the depth of all bridge foundations. For one specific site, RI, PS and SE methods were utilized and their effectiveness in determining unknown bridge foundations were evaluated and compared. The major objectives of the proposed study are:

- To determine the unknown foundation depth of bridge foundation using resistivity imaging.
- To investigate the applicability of RI for determining unknown bridge foundation depths
- To determine unknown foundation depth using Parallel Seismic (PS) and Sonic Echo (SE) method.
- To compare and propose best methods for determining unknown foundation depth.

1.4 Organization

A brief summary of the chapters included in this thesis is presented in the following paragraphs.

Chapter 1 presents the significance of the subject matter and statement of purpose. Chapter 2 presents literature review of different NDT approaches and case studies to determine unknown foundation depth. This chapter also includes the concept of electrical resistivity imaging and a brief review of available array methods.

Chapter 3 is devoted to field studies which describe the field investigation program for the unknown foundation determination using 2D and 3D resistivity imaging. The field investigation program using Parallel Seismic and Sonic Echo method is also included in this chapter.

Chapter 4 describes comprehensive analysis of all electrical resistivity test results for unknown foundation determination at three different locations. The test results for Parallel

seismic and Sonic echo test is also included and compared with RI test results. The test results are also compared with the actual foundation depth.

Chapter 5 includes a summary of accomplished work and the main conclusions.

CHAPTER 2

LITERATURE REVIEW

2.1 Introduction

Many of the older bridges in the United States have no original contract documents available. About 26,000 bridges in the national bridge inventory are rated as scour critical have unknown foundation condition that have no information is available regarding the type, depth, geometry or materials. However, state bridge engineers cannot provide funds for the required investigation with conventional excavation, coring or boring methods to determine unknown bridge foundation depth with normal maintenance operations at required funding levels (Olson et al., 1998). Non Destructive testing (NDT) method is used for a number of years to investigate the integrity of the structure. Recently these methods are used to determine the unknown foundation depth. However, determining the unknown foundation depth from a existing structure differs from conventional NDT method as this foundation top are not accessible (Gassman and Finno, 1999).

An unknown bridge foundation material property differs from the surrounding geotechnical and hydrological environment. The foundation materials may be steel, wood, concrete or masonry. The bridge foundation shape may be that of a footing, a pile or a combination of the two. The differing materials properties and geometries of foundations are the most important factors to be considered to nondestructively determine unknown foundation. A wide range of possible technologies are available in the literature to determine unknown foundation depth. However, the selection of specific method depends on its utility and the type

of the foundation to be tested. Site accessibility also has an impact on the selection of the NDT methods to determine foundation depth.

2.2 Non Destructive Test for Unknown Foundation

Conventionally excavation, coring and boring excavation is the most positive means to determine the unknown foundation depth and type. However, this excavation process is expensive, destructive and limited in their application to determine unknown foundation depth. On the other hand NDT methods provide cost effective and non destructive solution to determine unknown foundation depth. A wide range of NDT test includes stress waves, electrical/electromagnetic, magnetic and gravity measures are available to determine the depth of the foundation. The Sonic Echo/Impulse Response method, Ultraseismic Method, Dispersive/Bending Wave method, Parallel Seismic method, Ground Penetrating Radar (GPR), Magnetometer test and Induction methods are commonly used NDT test to determine the Unknown Foundation Depth. These methods are discussed in the following section.

2.2.1 Sonic Echo (SE)/Impulse Response (IR) Method

The Sonic Echo/Impulse Response (SE/IR) method was developed for testing the integrity and length of columnar shaped deep foundations such as drilled shafts and driven piles. These two methods are widely used for the determination of depth of columnar structure shapes such as timber piles, concrete piles and drilled shafts. SE method can also be effectively utilized to determine the depth of shallow foundation, wall shaped abutments and piers. SE/IR method is based on the principal that stress waves will reflect from significant changes in stiffness. This method involves measuring the velocity of wave travel in a known structure. Tracking the reflection event from the structure, the depth of the bridge of foundation can be determined by placing an accelerometer at the top of the structure (Olson et al., 1998). The schematic diagram of SE method is presented in Figure 2.1.

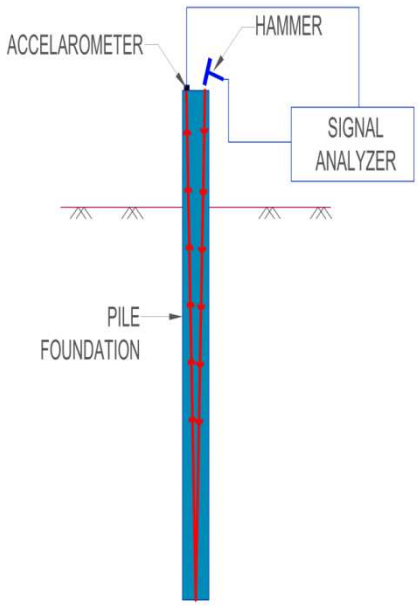

Figure 2.1 Sonic Echo/Impulse response method (redrawn after Olson et al., 1998[b])

The Sonic Echo method includes impacting at the top of the bridge foundation with a hammer to generate compressional wave. The compressional wave travels through the foundation along its length of the columnar structure. The compressional wave energy reflects back to the surface form the change in stiffness, cross-sectional area, and density which are known as change in impedance. Impedance is the product of velocity, mass density and cross sectional area of the foundation structure.

Impedance = velocity x mass density x cross sectional area…… (2.1)

Drill shaft foundations may have neck, bulb or break as construction defects. Neck is a construction defect that have lower cross sectional area results lower impedance. On the other hand, bulb is the construction defects where the foundation has higher cross sectional area that has higher impedance. The arrival of the reflected stress wave is sensed by accelerometer placed at the top of the pile foundation. For the data analysis, time domain is utilized in the Sonic Echo test and frequency domain is utilized in the Impulse Response test (Olson et al.

1998). The Sonic Echo/Impulse response method is mostly applicable to columnar structure on drill shafts or deep foundations that are exposed above the ground or water. Limitation of this method is it requires direct instrumentation to the foundation element. As a rule of thumb, when embedded length to diameter ratios are greater than 20:1 to 30:1 in stiffer soils, no bottom echoes are identifiable due to the excessive damping of the compression wave energy. (Olson et al., 1998; Briaud et al, 2002).

Steel H-pile have higher surface area compared to the cross sectional area. Due to higher surface area, the stress wave is damped and weakens throughout the length of the pile. As a result, SE method may not be suitable for the determination of steel H-pile length. Olson et al. (1998) studied different unknown foundation utilizing the SE/IR method. The investigation results are presented in Table 2.1

Table 2.1 Summary of Sonic Echo/Impulse Response Test Results (Olson et al., 1998).

Bridge Location	Tested Unit	Substructure Type	Actual Depth (ft)	Predicted Depth (ft)
Golden (Colorado)	North Pier	Concrete Columns on shallow footings, connection breast wall	(42.8’ from top of beam down column to bottom of footing. Embedded depth of 14.8’	No success
Coors (Colorado)	Pier 4	Concrete Columns on shallow footing supported by steel piles	(31.1’ from top of beam down column to bottom of footing, steel piles are 25’ long, embedded, depth of 28.8’	No success

Table 2.1 - continued

Bridge Location	Tested Unit	Substructure Type	Actual Depth (ft)	Predicted Depth (ft)
Golden (Colorado)	North Pier	Concrete Columns on shallow footings, connection breast wall	(42.8’ from top of beam down column to bottom of footing. Embedded depth of 14.8’	No success
Coors (Colorado)	Pier 4	Concrete Columns on shallow footing supported by steel piles	(31.1’ from top of beam down column to bottom of footing, steel piles are 25’ long, embedded, depth of 28.8’	No success
	Pier 2	Concrete columns on shallow footings	(26’ from top of beam down column to bottom of footing). Embedded depth of 4.5’	No success
Franktown (Colorado)	Northeast Wing (Abutment)	Exposed timber piles	28’ embedded depth of 21'	29.8’ (SE tests) 27.9’ (IR tests)
	Middle pier	Cap on top of exposed timber piles	28’ embedded depth of 25'	23.8’ (SE tests) 23.2’ (IR tests)
Weld (Colorado)	West Pier	Massive Concrete abutment supported by steel piles	(6’ depth of abutment) Steel piles are 34.5’ long (1 ft in pile cap), embedded depth of 34’	6.6’ (SE tests) 6.5’ (IR tests) No success for steel pile length

Table 2.1 - continued

Bridge Location	Tested Unit	Substructure Type	Actual Depth (ft)	Predicted Depth (ft)
Alabama (Alabama)	Bent 4	Steel piles extending to the bottom of the superstructure	(39’ form ground surface to tip of pile)	No success
Old Bastrop (Texas)	Caisson	Two Circular columns connected by a breast wall supported by a bell shape concrete footing supported on a rectangular concrete footing	(38’ from top of columns to top of bell section, 16’ thick rectangular section). Embedded depth of 35’	35.9’ (upper columns, SE tests) no success for the bell and rectangular sections depth determinations
	Piles	Concrete Columns supported by a pile cap of concrete piles	(3’ thick pile cap, 32’ long concrete piles, embedded depth of 33.3’)	No success
New Bastrop (Texas)	Drilled Shaft	Concrete Columns supported by shafts	45’ long shaft, embedded depth of 38’	38’ (depth below grade, SE tests)

During the Sonic echo method, bottom echoes can be obtained for embedded length to diameter ratio of 20:1 for moist soil. However for soft soil, foundation depth can be measured for slenderness ratio up to 50:1. Impulse response tests will generally be useful when performed at the tops of piles and shafts as the resonance are clearest there. SE/IR method does not work

well when tests are conducted through more massive and complex members, such as beams, pile caps, smaller columnar piles and shafts. From modeling and field experience, the compressional wave energy is trapped in the larger element because of the impedance contrast. Presences of very hard soil or bedrock have the opportunity of loosing strength of the bottom echoes (Olson et al., 1998)

2.2.2 Dispersive Wave

Dispersive wave technology considers the change in shape of the stress wave or signals with the propagation through the materials. Dispersion of stress wave is an unavoidable phenomenon where a signal transmits at their velocities. Conventional signal analysis technologies for dispersive behavior are based on the Fourier transformation. During this method the relative phase angle for individual frequencies between two gage locations are measured. This relative phase is utilized to determine the time required for the frequencies to travel a known distance from where the phase velocity is determined (Stegman and Holt, 2000). Figure 2.2 presents the schematic set up and a typical example of the data from a 10.6 m long timber pile.

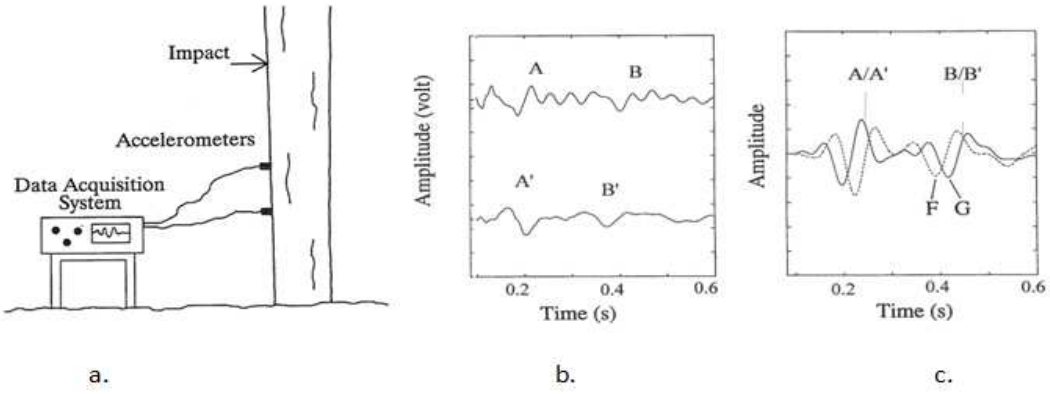

Figure 2.2 a. Schematic of Dispersive wave method, b. raw signal trace from a 10.6 m timber pile, c. Filtered two signal using Fourier transform and cross-sectional spectral method (Stegman and Holt, 2000).

The main advantage of the Dispersive wave method is, it require horizontal impact. Due to the horizontal impact, flexural stress wave forms that transmit through the structure. This advantage can be utilized to determine the unknown foundation depth that have elevated portion over the ground or over water. Stegman and Holt (2000) successfully utilized dispersive wave technologies to measure thickness and depth of a bridge abutment. Summary of the results are presented in Table 2.2. where test results are verified with the conventional boring.

Table 2.2 Summary of Dispersive wave results (Stegman and Holt, 2000).

Location	East Abutment Depth (Dispersive Wave)	East Abutment Depth (Conventional Boring)	West Abutment Depth (Dispersive Wave)	West Abutment Depth (Conventional Boring)
3 m Right of Centerline	1.8 m	1.2	3.6 m	4.2 m
Centerline	1.5 m		4.0 m	
3 m Left of Centerline	1.46 m		3.8 m	

Olson et al. (1998) performed dispersive wave test on a 25.5 ft steel H pile. The measured length using the dispersive wave test was found 26 ft. However, after driving, the pile had only 1 ft extended over the ground level and no test can be performed. Due to greater surface area of steel piles per unit length, the reflected dispersive wave energy cannot be utilized for the steel H-pile. The author also reported dispersive wave test for timber piles. Comparing to the actual pile length, 16 piles out of 26 piles had shown variation which ranged -11.8% to +8.7%.

2.2.3 Ultra Seismic Method

The Ultra Seismic Method was developed from the difficulties encountered by Sonic Echo and Dispersive Wave methods for complex structure. The working principal for Ultra Seismic Method is similar to sonic echo method but the data acquisition and processing unit use multiple channels. During the Ultra Seismic Method, the arrival and reflection of compressional and bending wave are analyzed and processed to determine the unknown foundation depth. Two types of Ultra Seismic test geometries are available. For 1D imaging and tracking the up going and down going waves, Vertical Profiling (VP) method is used. VP method can be run both in the columnar and tabular structure. During this method, the bridge column is hit at the top and resulting wave motion is recorded at regular interval. Typically three component of wave field is taken in to consideration to analyze the wave motion. On the other hand, for two dimensional imaging, Horizontal profiling test geometry is used. In this method, the source and receiver are located horizontally along the top of accessible substructure (Olson et al., 1998). Vertical profile test geometry is presented in Figure 2.3.

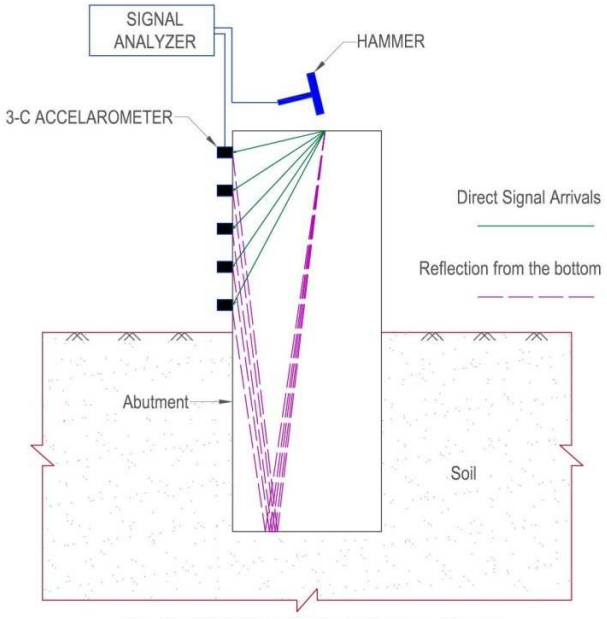

Figure 2.3 Ultraseismic test method with Vertical Profiling Geometry (redrawn after, Olson et al. 1998)

During Ultraseismic test, four types of stress wave are generated that includes longitudinal, torsional, surface and flexural waves. In the longitudinal wave, elements of the column extend and contract along the direction of the wave. In torsional wave, elements of the column remain at its original plane and try to rotate about its center. During the flexural or shear wave, axis of column move laterally perpendicular to its axis. Vertical impact in the bridge substructure produce compressional or longitudinal wave. On the other hand, horizontal impact on the substructure produce flexural wave. Both the longitudinal and flexural wave are utilized during the Ultraseismic method.

Olson et al. (1998) performed Ultraseismic method on seven bridge foundations to determine the unknown depth. The summary of the investigation result is presented in Table 2.3.

Table 2.3 Summary of Ultraseismic test (Olson et al., 1998)

Bridge Location	Tested Unit	Substructure Type	Actual Depth (ft)	Predicted Depth (ft)
Golden (Colorado)	North Pier	Concrete Columns on shallow footings, connection breast wall	(42.8' from top of beam down column to bottom of footing. Embedded depth of 14.8'	42.0' (P-wave) 42.9' (Flexural Wave) (from top of beam)
New Bastrop (Texas)	Drilled Shaft	Concrete Columns supported by shafts	45' long shaft, embedded depth of 38'	45' (from top of shaft) or 38' (from ground surface) (Flexural)

Table 2.3 - continued

Bridge Location	Tested Unit	Substructure Type	Actual Depth (ft)	Predicted Depth (ft)
Coors (Colorado)	Pier 4	Concrete Columns on shallow footing supported by steel piles	(31.1' from top of beam down column to bottom of footing, steel piles are 25' long, embedded, depth of 28.8'	31.1' (P-wave) 29.7 (Flexural Wave) 33.9' (Frequency from top of beam
	Pier 2	Concrete columns on shallow footings	(26' from top of beam down column to bottom of footing). Embedded depth of 4.5'	25.9' (Flexural Wave) (From top of beam)
Franktown (Colorado)	Northeast Wing (Abutment)	Exposed timber piles	28' embedded depth of 21'	Not successful
	Middle pier	Cap on top of exposed timber piles	28' embedded depth of 25'	23' (Compression) (from top of pile)
Weld (Colorado)	West Pier	Concrete wall on concrete footing supported by steel piles	(18.9' from top of wall to bottom of footing), steel piles are 25' long. Embedded depth of 34.6'	18' (from top of wall) (Flexural)
Alabama (Alabama)	Bent 4	Steel piles extending to the bottom of the superstructure	(39' form ground surface to tip of pile)	34'-35' (Compressional) 35' (flexural) (From ground surface)

Table 2.3 - continued

Bridge Location	Tested Unit	Substructure Type	Actual Depth (ft)	Predicted Depth (ft)
Old Bastrop (Texas)	Caisson	Two Circular columns connected by a breast wall supported by a bell shape concrete footing supported on a rectangular concrete footing	(38’ from top of columns to top of bell section, 16’ thick rectangular section). Embedded depth of 35’	Two depths: 37’ (from top of bell section and 18.6’ (from top of bell section) Both depths are from flexural waves
New Bastrop (Texas)	Drilled Shaft	Concrete Columns supported by shafts	45’ long shaft, embedded depth of 38’	45’ (from top of shaft) or 38’ (from ground surface) (Flexural)

2.2.4 Parallel Seismic Test Method

Parallel Seismic (PS) method is a borehole based method. This method has the widest range of application of any of the methods for determining unknown foundation bottom depths regardless of depth, substructure type, geology, and materials. With the aid of using geophone and hydrophones, foundation bottom with wide range of conditions can be determined. In parallel seismic method, both the compressional and shear wave can be used as generated by vertical and horizontal impact (Olson et. al, 1998). Parallel Seismic Test Method is based on the principal that an impact on the exposed structure generates wave energy that travel down the structure. This traveling wave transmits through the soil adjacent to the foundation and can be traced by placing sensors parallel to the structure through nearby parallel boring. Depth of the foundation is determined with the variation of velocity of the wave traced by the sensors. The PS method was developed to determine the unknown foundation depth (Olson et al., 1998). The

Parallel Seismic (PS) test is performed by impacting the structure with an instrumented hammer to the exposed surface of the foundation. The impact can be done at the top or at the side of the exposed structure. Due to the hammer impact, compressional p-wave generates through the structure. These generated wave travels down along the structure and couple in to the surrounding soil. The coupled compressional wave in the soil can be traced by a nearby hydrophone or geophone receiver. This hydrophone receiver is typically suspended in a water filled cased bore hole parallel to the foundation. The repeated impact on the structure with alternate receiver depth is stored in the signal analyzer. The stored data is utilized to create a plot of receiver signal arrival time versus depth. The analysis of unknown foundation depth is done from the plot. The PS test method is illustrated in Figure 2.4.

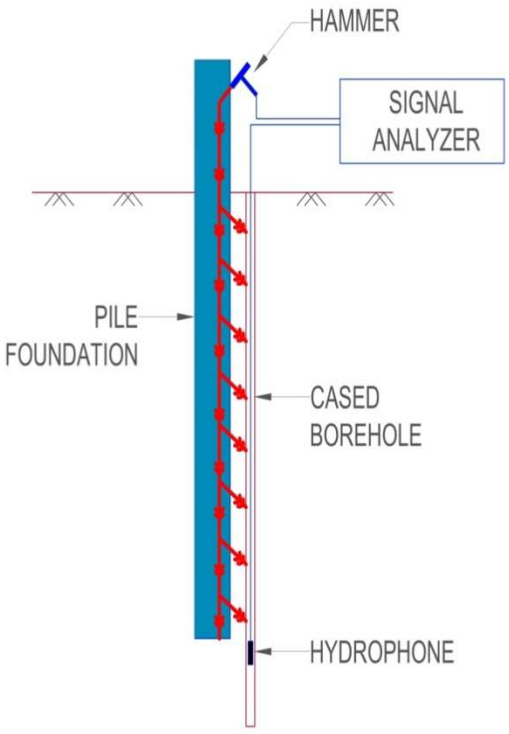

Figure 2.4 Parallel Seismic Method (Redrawn after Olson et al, 1998)

The tip depth of a foundation is determined by an inflection point in the arrival time versus depth curve, along with a sharp drop in signal amplitude. Diffraction of wave energy from the foundation bottom is also considered as an indication of foundation depth. Thus the depth of foundation from PS test can be determined from the breaks in slope of the lines in a plot of depth versus recorded time plot, drop in energy amplitude below the foundation and diffraction of wave energy at the bottom of the foundation (Sack & Olson, 2009). The waveforms are observed clear and regular to identify the first arrival time. However in saturated soil the waveforms are complicated and it become difficult to identify the first arrival time (Huang and Chen, 2007)

Olson et al., (1998) performed PS test at three concrete foundations at Old and New Bastrop bridges in Texas (that include concrete pile, caisson and drilled shaft foundation), a concrete pile cap on steel H-pile foundation at Coors bridge in Colorado and a steel pile bridge in Alabama. The test results and comparison of predicted vs. actual foundation depth is presented in Table 2.4.

Table 2.4 Summary of Parallel Seismic Test Results (Olson et al., 1998).

Bridge Location	Tested Unit	Substructure Type	Actual Depth	Predicted Depth (ft)
Coors (Colorado)	Pier 4	Concrete columns on shallow footing supported by steel piles.	28.8’	27’ (Geophone) 29’ (Hydrophone)
Alabama (Alabama)	Bent 4	Steel piles extending to the bottom of the superstructure	East Pile: 39’ Middle Pile : 39’	East Pile: 30’ (Geophone) Middle Pile: 31.6’ (Geophone) 34.6’ (Hydrophone)

Table 2.4 - continued

Bridge Location	Tested Unit	Substructure Type	Actual Depth	Predicted Depth (ft)
Coors (Colorado)	Pier 4	Concrete columns on shallow footing supported by steel piles.	28.8’	27’ (Geophone) 29’ (Hydrophone)
Alabama (Alabama)	Bent 4	Steel piles extending to the bottom of the superstructure	East Pile: 39’ Middle Pile : 39’	East Pile: 30’ (Geophone) Middle Pile: 31.6’ (Geophone) 34.6’ (Hydrophone)
Old Bastrop (Texas)	Caisson	Two circular columns connected by a breast wall supported by a bell shape concrete footing supported on a rectangular concrete footing	35’	Borehole 1: 35.3’ (Geophone) 38.3’ (Hydrophone) Borehole 6: 35’ (Geophone)
	Piles	Concrete columns supported by a pile cap of concrete piles	33.3’	32’ (Geophone) 32’ (Hydrophone)
New Bastrop (Texas)	Drilled Shaft	Concrete Columns supported by Shafts	38’	35.3’ (Geophone) 38.3’ (Hydrophone)

Data interpretation in the Parallel seismic test can be complicated with high variable of soil condition (Finno et al., 1997). This method required a drilled cased bore hole to protect the tools and keep the bore hole open. This can be costly for river environment of bridges. Sack and Olson (2009) presented an alternative solution of cased bore hole. In the alternate method, a combination of CPT rig with Geophone should be used. Using this approach, the subsurface data can be achieved during the PS test.

2.2.5 Ground Penetrating Radar (GPR)

Ground Penetrating Radar (GPR) is used to determine the presence of reinforcement in the foundation or abutment, to verify the presence of footing in the foundation and anomalies in the concrete. It can also be used to find dimensions and depths below grade of buried footings. GPR transmit UHF and VHF frequencies (10 MHz to 2 GHz) at a very low radiated power (0.6-100 milli-watts). During the GPR, antennas transmit electromagnetic energy and receive reflections from material that have dielectric contrast. The GPR conceptual drawing is illustrated in Figure 2.5.

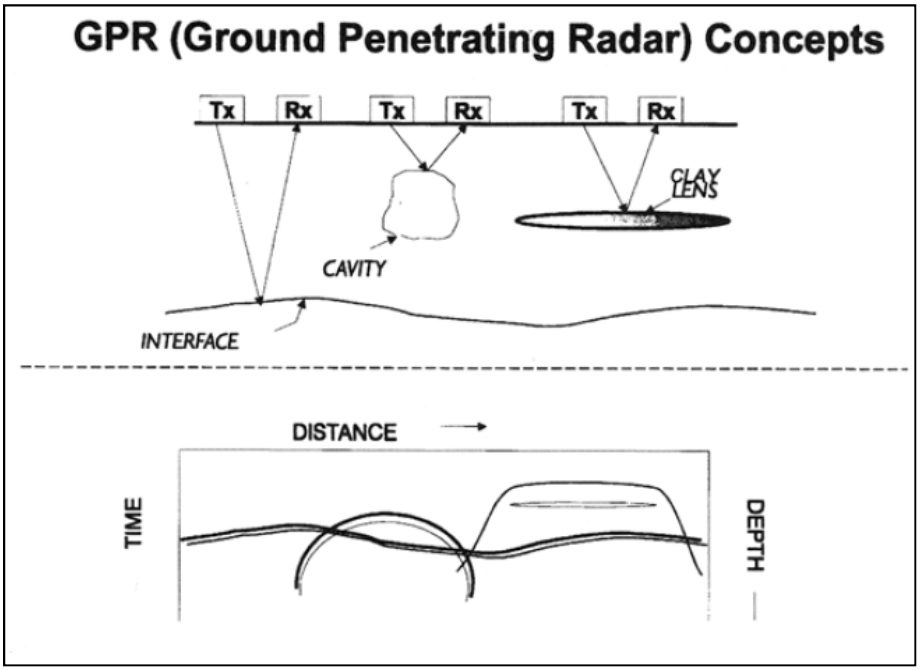

Figure 2.5 GPR concepts (Stegman and Holt, 2000).

During the GPR, the depth of penetration of electromagnetic energy and resolution are dependent on the antenna frequency, subsurface dielectric permittivity and conductivity. With the increase in penetration depth, the signal weakens and resolution goes down. With lower frequency, higher penetration depth can be achieved. On the other hand, resolution will be higher with lower penetration depth and higher frequency. The radiation pattern is also greatly affected by Dielectric Permittivity and Electrical conductivity.

Dielectric permittivity is a dimensionless measure of the capacity of a material to store a charge when an electric field is applied. Greater radar penetration takes place with lower dielectric constant. Electrical conductivity is the inverse of the resistivity of the material. With higher electrical conductivity, deeper radar signal penetration becomes difficult. Thus conventional resistivity testing is a good indication of sites suitability for GPR (Stegman and Holt, 2000).

Soil dielectric constant is a function of moisture content of soil. With increase in moisture content, the dielectric content of soil increase. This results in a decrease in radar velocity or longer travel paths through the same thickness of soil. An increase in water content also increase the electrical conductivity of soil. This increase in electrical conductivity result reduced depth of penetration of radar signal. Thus environmental factors such as salt water, conductive soils, ground moisture condition and buried electrical lines in the ground effects the radar signal. GPR suits well with sandy soil and soil with low conductivity (Olson et al., 1998).

Olson et al. (1998) utilized GPR to determine the unknown foundation length. During this study, the author performed GPR at 6 different bridge foundation and successfully determined only one foundation. During this study, the author summarized that the radar signals were mostly affected by noise and penetration are restricted in clayed soil.

2.2.6 Magnetometer Test

The earth is a magnet and the rebars in the foundation is magnetized under the earth magnetic field which will act as a magnet. With the aid of using magnetometer, the presence of the rebar can be detected by measuring the induced magnetic field. Therefore the pile length can be determined based on the length of the rebar. During this method, a parallel non metallic pipe is installed with the pile foundation and magnetometer is inserted. Rebar has a great length to diameter ratio. The induced magnetic field is relatively uniform within the length of the rebar. However, considerable change in the magnetic field is observed at the bottom of the rebar. Thus this change is considered as bottom of the rebar and the length of the pile foundation is determined (Yu et. al., 2007). The schematic diagram of magnetometer for pile length determination is presented in Figure 2.6

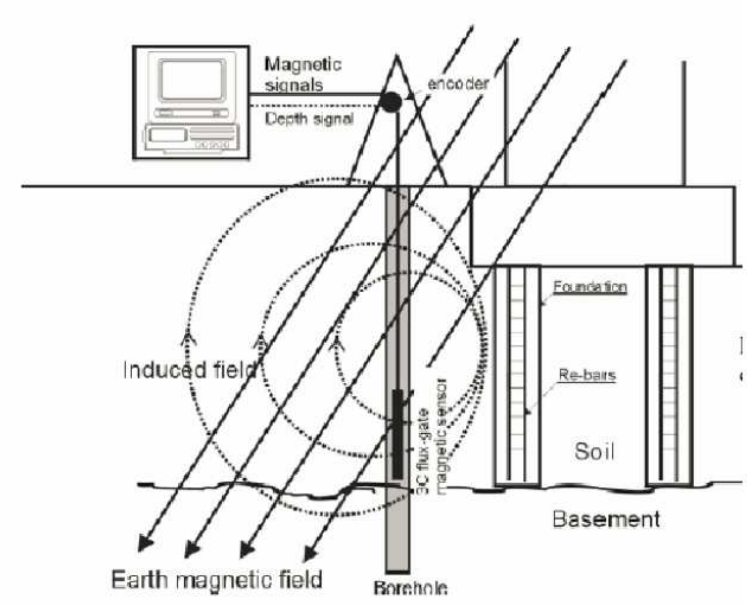

Figure 2.6 Schematic of Magnetometer for Pile length determination (Yu et al., 2007)

A PVC pipe is generally installed parallel to the pile foundation to facilitate the insertion of the magnetometer. The casing is filled with water. Magnetometer is inserted in the casing and continuous data is collected along the length of the casing.

Yu et al. (2007) performed a magnetometer testing on two pile foundation of an existing building in Georgia. From the investigation result the magnetometer had shown the trend of the reinforcement change along depth. From the investigation result the pile foundation length was determined as 60 ft. The pile length was verified with Parallel seismic method and the length determined using parallel seismic method was 65 ft. Thus magnetometer test results from these two methods had shown good consistency. However, this can only be effective for the determination of steel piles and concrete pile that have reinforcement. This test cannot be utilized for timber pile and masonry structure due to absence of any steel reinforcement.

2.2.7 Induction Method

The induction field method is typically used for the determination of the depth of steel piles and reinforced concrete piles. Induction method requires a non-ferrous cased boring. This method works well in soils having uniform conductivity. During this method, AC current flow is impressed into a steel pile or in the rebar of Reinforced concrete pile. The flowing current couples into the subsurface and return through an electrode. This return electrode can be another pile or a piece of rebar driven into the ground. A receiver coil is suspended in a nearby boring is used as a sensor of the magnetic field induced by the alternating current flow in the pile. Steel pile and Reinforced concrete pile depth can be measured from this method. Figure 2.7 present the schematic diagram of Induction field method.

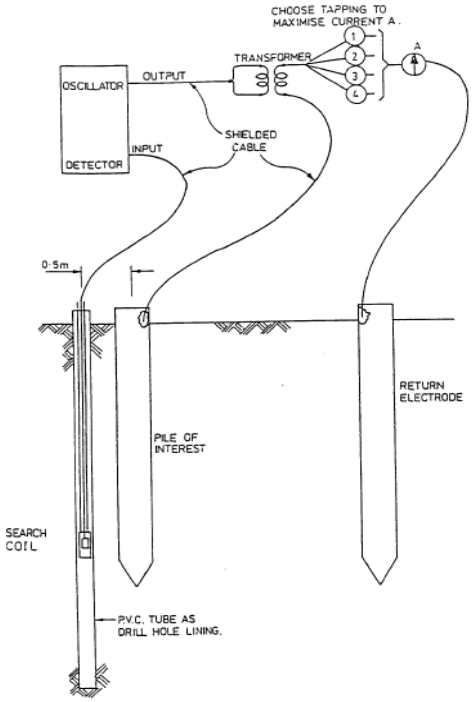

Figure 2.7 Induction Field Method (Olson et al., 1998)

By plotting the magnitude of the induced voltage vs. the depth of the coil, the depth of the pile can be measured. When the search coil is below the bottom of the foundation, the measured voltage tends to stabilize at a low value. A tangent point to the linear portion of the curve is used to estimate the foundation depth. This method can only be utilized for the determination of steel or reinforced concrete pile structure which can be electrically connected to rebar or other metal that can be accessed at the surface (Olson et al., 1998; Robinson and Webster, 2008). However, the test result affect by the presence of ground water. This method does not work for unreinforced concrete, masonry or timber.

2.3 Resistivity Imaging

Electrical resistivity is one of the oldest and popular geophysical techniques in electrical exploration. This technique can be utilized to produce images of the subsurface with the aid of automated data acquisition system and user friendly software. The first resistivity survey was

conducted by Schlumberger brothers during 1920. Now a days, resistivity is one of the primary methods in measuring the electrical resistive properties of soil. Electrical resistivity is measured by placing four electrodes in contact with the soil or rock. (Maganti, D., 2008).

Electrical Resistivity technology has recent advancement with the increased sophistication of electrical hardware and software. Two methods of subsurface imaging using electrical resistivity were available. The first method, Electrical sounding was used to investigate depth which provides information of one dimensional vertical profile with limited lateral variations. On the other hand, Electrical trenching generated a lateral profile but limited to a constant depth (Telford et al. 1990).

Multi-electrode systems have the facility to conduct both electrical sounding and Electrical trenching simultaneously. Using today's advanced instruments to acquire the data as a set of sounding comprising a two dimensional cross-section or resistivity profile of the subsurface. On the basis of the distribution resistivity profile, an accurate interpretation of the subsurface geologic setting can be made (Maganti, D., 2008).

Electrical Resistivity Imaging is a non invasive geophysical technique that can provide a subsurface resistivity image. This imaging can be used for surface exploration, subsurface characterization and monitoring.

2.3.1 Theory of Resistivity

Electrical Resistivity Survey is conducted to determine the resistivity distribution of soil volume. Electrical current is supplied to the soil and resulting potential difference is measured. Measured potential difference pattern provides information on the subsurface condition and their electrical properties. (Kearey et. al., 2002). Electrical resistivity of the soil is considered as a proxy for the variation of soil properties (Banton et. al., 1997). For a simple body, the resistivity ρ (Ω m) is defined as

$\rho = R(A/L)$ …… (2.2)

Where R is the electrical resistance, L is the length of the cylinder (m) and A is the cross sectional area (m^2).

The electrical resistance of a cylindrical body is defined by the Ohm's law.

$R = V/I$…… (2.3)

Here, V is the potential difference measure in Volt and I is the current which is typically measured in Ampere. The conductivity (σ) is term reciprocal of resistivity.

Where,

$\sigma = 1/\rho$ …… (2.4)

In a homogeneous and isotropic half space, electrical equipotentials are hemispherical as shown in Figure 2.8 (Samouëlian et al., 2004). The current density J (A/m^2) is calculated for all the radial directions with,

$J = I/2\Pi r^2$…… …… (2.5)

Here, $2\pi r^2$ is surface of a hemispherical sphere of radius r. The potential V can be expressed as,

$V = \rho I/2\Pi r$…… (2.6)

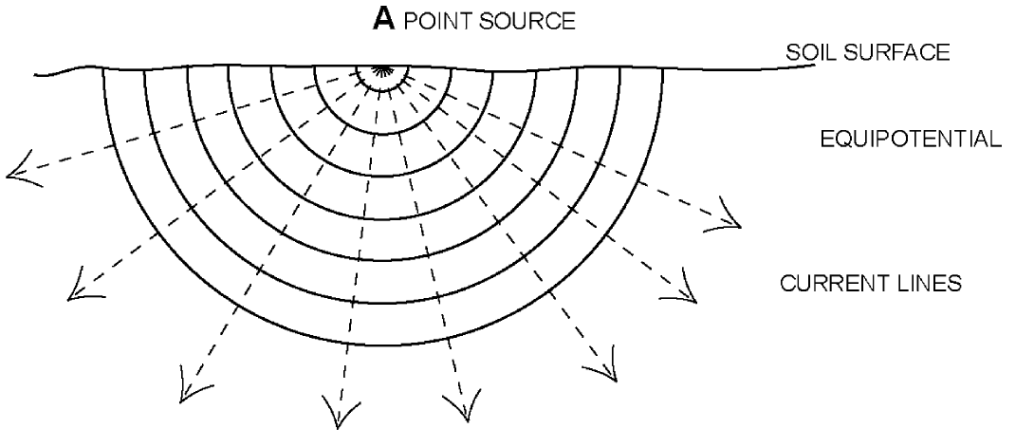

Figure 2.8 Distribution of current flow in a homogeneous soil (Samouëlian et al., 2004)

For the measurement of electrical resistivity, four electrodes are required. Two electrodes A and B in between the four electrodes are known as current electrode. The other two electrodes M and N are known as potential electrode. The current electrodes inject the current in the soil, resulting potential difference are measured by the potential electrodes. Figure 2.9 presents the equipotentials and current lines for a pair of current electrodes A and B on a homogeneous half-space.

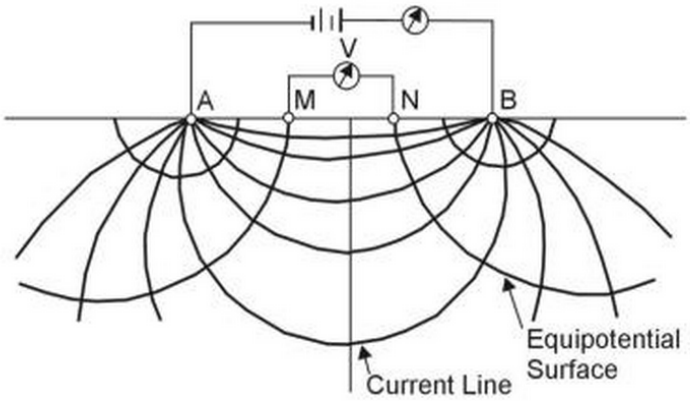

Figure 2.9 Equipotentials and current lines for a pair of current electrodes A and B (www.cflhd.gov).

The potential difference between the M and N is given by the equation,

$$\Delta V = \frac{\rho I}{2\Pi}[1/AM - 1/BM - 1/AN + 1/BN] \quad \text{(2.7)}$$

Where AM, BM, AN and BN are geometrical distance between the A and M electrode, B and M electrode, A and N electrode and B and N electrode respectively. The electrical resistivity is then calculated by the expression,

$$\rho = \Delta V/I[6\,2\Pi/(1/AM - 1/BM - 1/AN + 1/BN)] \quad \text{(2.8)}$$

or,

$$\rho = {}^{K\Delta V}/_{I} \quad \text{(2.9)}$$

Here, K is the geometrical coefficient that depend on the arrangement of A, B, M and N.

2.3.2 Variation of Electrical Resistivity as a Function of Soil Properties

The electrical resistivity is a function of different soil properties. Electrical resistivity of soil depends on the nature of the solid constituents (particle size distribution, mineralogy) arrangement of the voids (porosity, pore size distribution, connectivity) degree of water saturation (water content), electrical resistivity of the fluid (solute concentration) and temperature. The air medium act as an insulator which is infinitively resistive, the water solution resistivity is a function of the ionic concentration. The electrical resistivity of the solid grains is related to the electrical charges density at the surface of the soil particles. The electrical resistivity of soil is dependent on the soil properties but it varies with different ways and extent (Samoue¨lian et. al., 2004). The electrical resistivity for soil mapping had shown large range of values. The electrical resistivity had range from 1 Ω m for saline water to 10^5 Ω m for dry soil over crystalline rocks as shown in Figure 2.10 (Samouëlian et al., 2004).

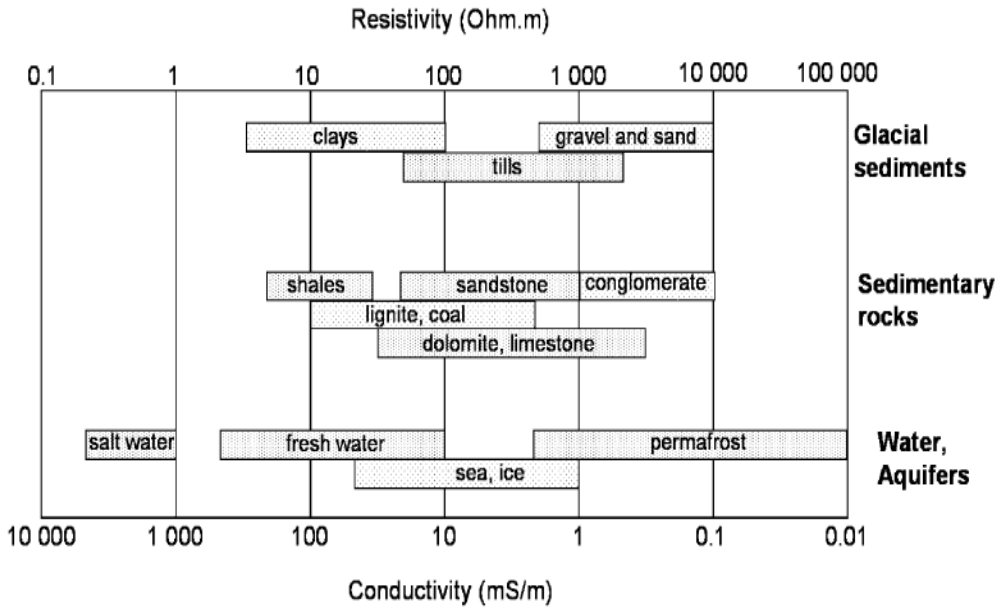

Figure 2.10 Typical ranges of electrical resistivity (Samouëlian et al., 2004).

2.3.3 Two Dimensional Resistivity

A two-dimensional multi-electrode array provides two dimensional vertical picture of the sounding medium. In 2D resistivity imaging, current and potential electrodes are maintained at a regular fixed distance from each other and are progressively moved along a line at the soil surface. At each step, one measurement is recorded. The set of all measurement at this first inter electrode spacing provides a vertical profile of resistivity values. The inter-electrode spacing is increase to n=2 and the second measurement is done. This process with increasing the factor for n is repeated until the maximum spacing is reached. The depth will be large with larger n values. The 2D resistivity imaging technique is presented in Figure 2.11 (Samouëlian et al., 2004).

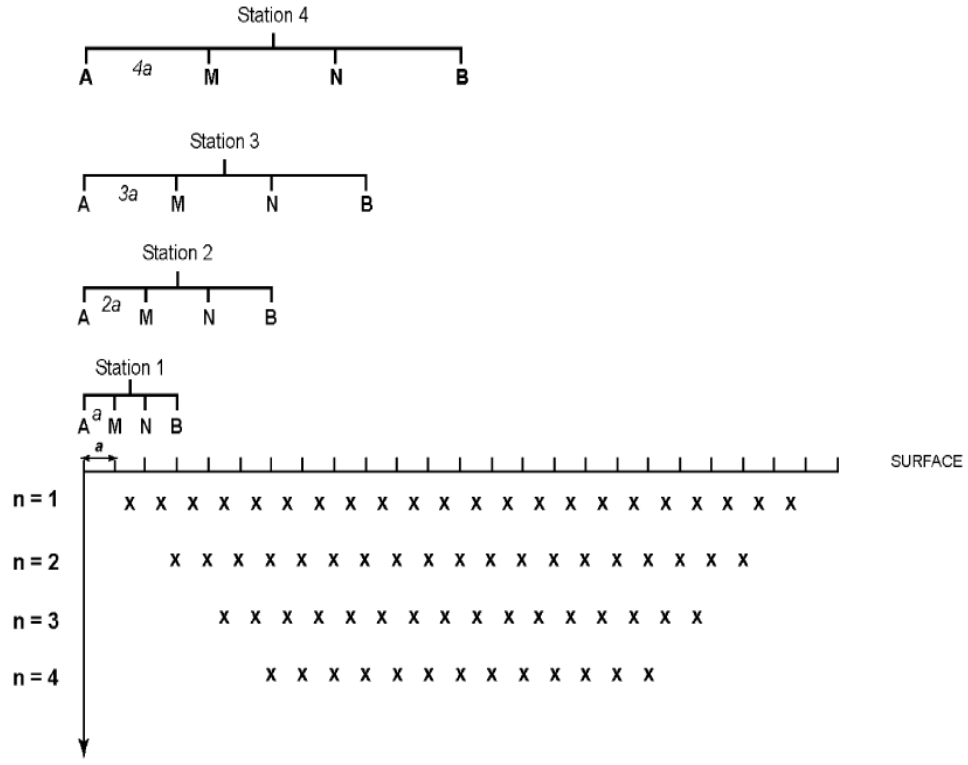

Figure 2.11 Establishment of a 2D resistivity imaging pseudo-section (Samouëlian et al., 2004)

The distribution of current is depends on the resistivity contrast of the medium. The depth of the investigation from the spacing is called the pseudo-depth and then the data are arranged in 2D pseudo-section plot. 2D pseudo-section plot gives simultaneous display of both horizontal and vertical variation of resistivity. In the conventional graphic representation, each measured value at the intersection of two 458 lines through the centers of the quadripole. Each horizontal line is then associated to the n value which gives the pseudo-depth of investigation (Samouëlian et al., 2004).

2.3.4 Electrode Array Configurations

Several array configurations are available based on the respective position of the potential electrodes and on the current electrodes. Wenner, Wenner-Schlumberger, dipole-

dipole, pole-pole & pole-dipole are the most commonly used array configurations as presented in Figure 2.12. Geometrical factor k depends on the geometrical configuration.

		Electrodes array	K
2D	Wenner	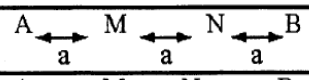	2πa
	Wenner-Schlumberger	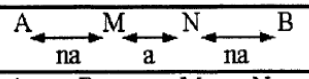	πn(n+1)a
	Dipole-Dipole	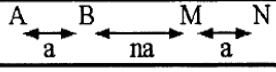	πn(n+1)(n+2)a
	Pole-Pole	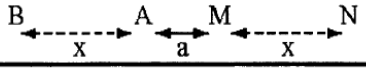	2πa
	Pole-Dipole *Forward*	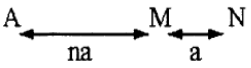	2πn(n+1)a
	Reversed	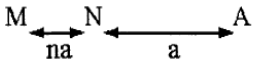	

Figure 2.12 Different array configuration for 2D resistivity Imaging (Samouëlian et al., 2004).

The array configurations have significant influence on the resolution, sensitivity and depth of investigation (Samouëlian et al., 2004). The sensitivity of the array to horizontal and vertical heterogeneities, depth of investigation, horizontal data coverage and signal strength of different array configurations are summarized in Table 2.5. The median depth of investigation for the different array and total length is presented in Table 2.6.

Table 2.5 Characteristics of Different 2D array configuration (Samouëlian et al., 2004)

	Wenner	Wenner-Schlumberger	Dipole-Dipole	Pole-Pole	Pole-Dipole
Sensitivity of the array horizontal structures	++++	++	+	++	++
Sensitivity of the array vertical structures	+	++	++++	++	+
Depth of investigation	+	++	+++	++++	+++
Horizontal Data Coverage	+	++	+++	++++	+++
Signal Strength	++++	+++	+	++++	++

The labels are classified form (+) to (++++), equivalent at poor sensitivity to high sensitivity for the different array configurations.

Table 2.6 Different median depth (Ze) and Length (L) covered by each array (Loke M. H., 1999)

Array type		z_e/a	z_e/L
Wenner alpha		0.519	0.173
Dipole-dipole	n = 1	0.416	0.139
	n = 2	0.697	0.174
	n = 3	0.962	0.192
	n = 4	1.220	0.203
	n = 5	1.476	0.211
	n = 6	1.730	0.216
Equatorial dipole-dipole			
	n = 1	0.451	0.319
	n = 2	0.809	0.362
	n = 3	1.180	0.373
	n = 4	1.556	0.377
Wenner - Schlumberger			
	n = 1	0.52	0.173
	n = 2	0.93	0.186
	n = 3	1.32	0.189
	n = 4	1.71	0.190
	n = 5	2.09	0.190
	n = 6	2.48	0.190
Pole-dipole	n = 1	0.52	
	n = 2	0.93	
	n = 3	1.32	
	n = 4	1.71	
	n = 5	2.09	
	n = 6	2.48	
Pole-Pole		0.867	

2.3.4.1 Wenner Method

Wenner Array is consisting of four electrodes in a line with equal spacing. Many early 2-D survey were carried out with this array. It is best suited for profiling because only one

electrode is moved for measurements. Figure 2.13 presents the sensitivity plot of the array. (Loke M. H., 1999)

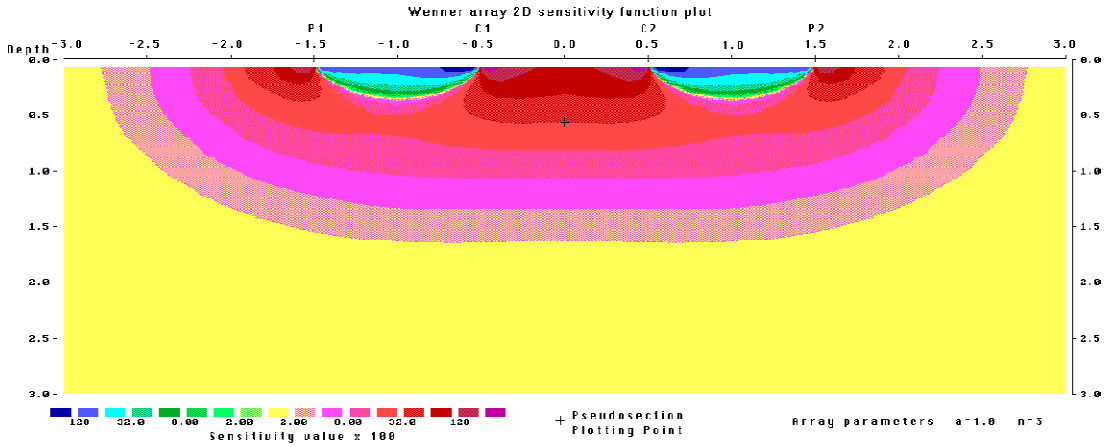

Figure 2.13 Sensitivity plot for Wenner Array (Loke M. H., 1999)

Wenner array is relatively sensitive to vertical changes in the subsurface resistivity below the center of the array. However, it is less sensitive to horizontal changes. For Wenner array has moderate depth of investigation where the median depth of investigation is approximately 0.5 times the “a” spacing used. The signal strength in a array is inversely proportional to the geometric factor used to calculate the apparent resistivity. For this array the geometric factor is 2πa which is relatively smaller. As a result, this array has better signal strength. One disadvantage of this method is poor horizontal coverage as the electrode spacing is increased. (Loke M. H., 1999).

2.3.4.2 Wenner Schlumberger Method

Wenner Schlumberger Method is relatively new method in electrical resistivity imaging surveys. This is a modified form of Schlumberger array where the electrodes can be spaced with a constant spacing. The sensitivity pattern for the Wenner Schlumberger method is presented in Figure 2.14. There are slight variation in the sensitivity patterns of Schlumberger array and Wenner array.

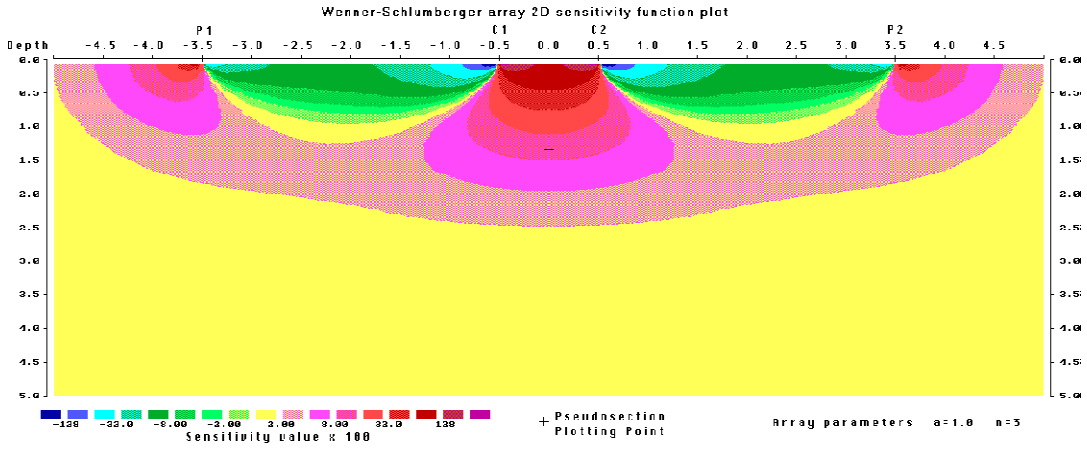

Figure 2.14 Sensitivity plot for Wenner Schlumberger Array (Loke M. H., 1999)

The signal strength of Wenner array is very high comparing to other method. For Schlumberger method the signal strength is in between Wenner array and dipole-dipole array. Comparing to Wenner array, the median depth of investigation (with same distance between the outer current electrode) is about 10% higher for Schlumberger array (Maganti, D., 2008)

Comparing to the Wenner array, Wenner-Schlumberger array has a slightly better horizontal coverage (Loke M. H., 1999). The pseudosection data pattern for the Wenner and Wenner-Schlumberger arrays are presented in Figure 2.15.

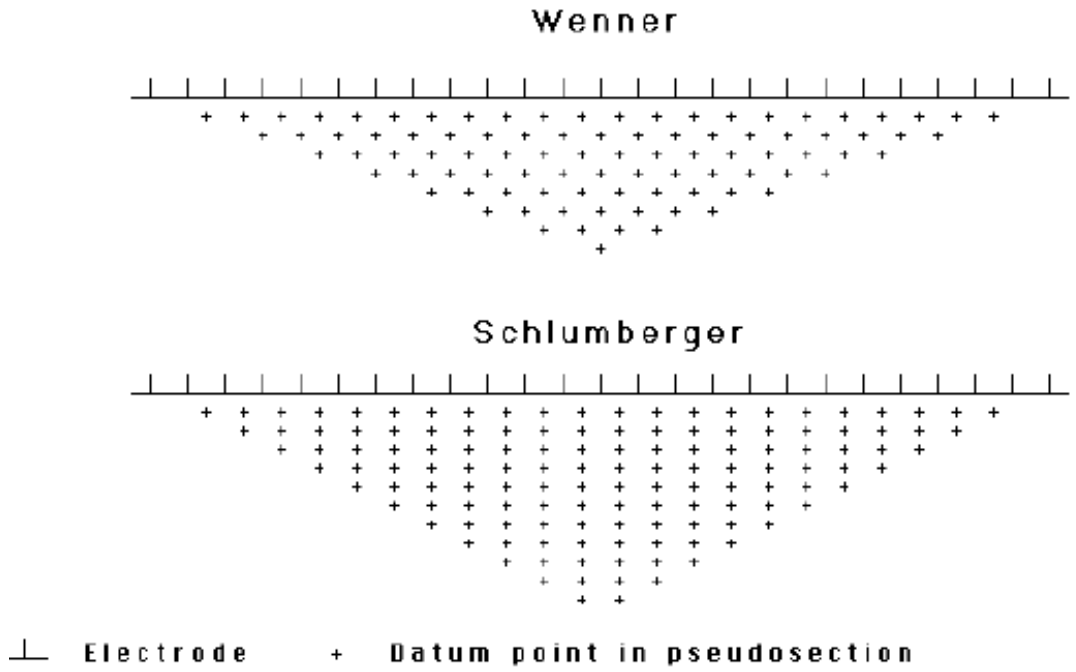

Figure 2.15 Pseudosection data pattern for the Wenner and Wenner Schlumberger arrays (Loke M. H., 1999)

2.3.4.3 Dipole-Dipole Method

The Dipole-Dipole array is the most convenient in the field. This method is suitable for for the work over large areas and larger spacing's between the electrodes. Dipole-Dipole array provides highest resolution and most sensitive to vertical resistivity boundaries. However, data collected from Dipole-Dipole array can be effected by near surface resistivity variations (Maganti, D., 2008). The spacing of electrodes in Dipole Dipole array is selected based on the desired depth of penetration, required resolution and type of array. Electrode spacing and dipole separation are constant for each traverse (n) and increases with successive traverse. With higher electrode spacing, greater penetration depth can be achieved but with poor resolution. The sensitivity plot for Dipole Dipole array is presented in Figure 2.16.

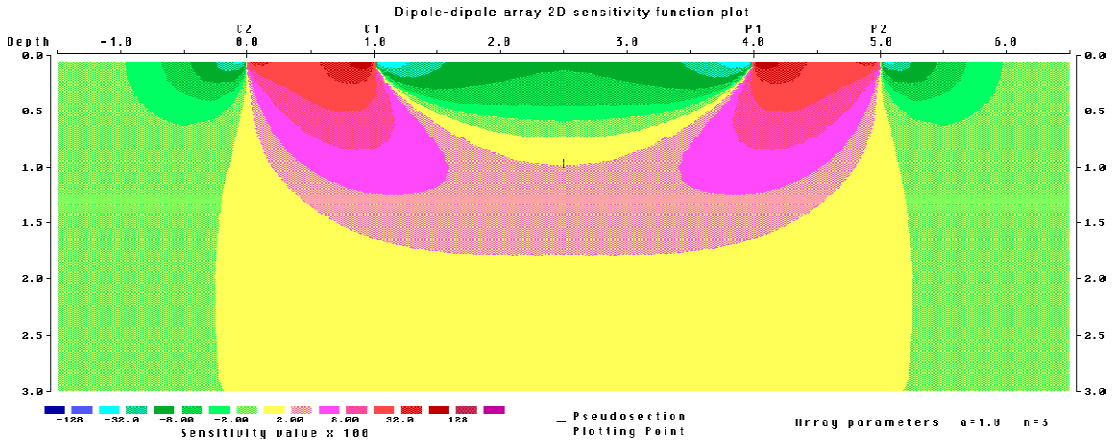

Figure 2.16 Sensitivity plot for Dipole Dipole Array (Loke M. H., 1999)

Largest sensitivity value is located below the current electrode pair and potential electrode pair in the function plot. This array is most sensitive to resistivity changes between the electrodes in each dipole pair. The sensitivity contour pattern is almost vertical in the plot. Thus the dipole dipole array is very sensitive to horizontal changes in resistivity but relatively insensitive to horizontal changes in resistivity which means, it is good in mapping vertical structure but relatively poor in mapping horizontal structures. This array has a shallower depth of penetration compared to Wenner array. However, it provides better horizontal resistivity data than the Wenner method (Loke M. H., 1999)

2.3.4.4 Pole Pole Method

Pole-pole array is not as widely used as the Wenner, dipole-dipole and Schlumberger arrays. In the ideal pole pole array, only one current and one potential electrode exist. However, second current and potential electrodes must be placed at a distance which should be more than 20 times the maximum separation between first pair of current and potential electrodes. In the dipole dipole array potential electrodes are placed at large distance. As a result, it may effected by large amount of telluric noise that can severely degrade the quality of the measurement. Dipole dipole this array is mainly used in surveys where relatively small electrode

spacing (less than a few meters) are used. This array has the widest horizontal coverage and the deepest depth of investigation. However, it has the poorest resolution, which is reflected by the comparatively large spacing. It is popular in some applications such as archaeological surveys (Loke M. H., 1999). The sensitivity diagram for pole pole method is presented in Figure 2.17.

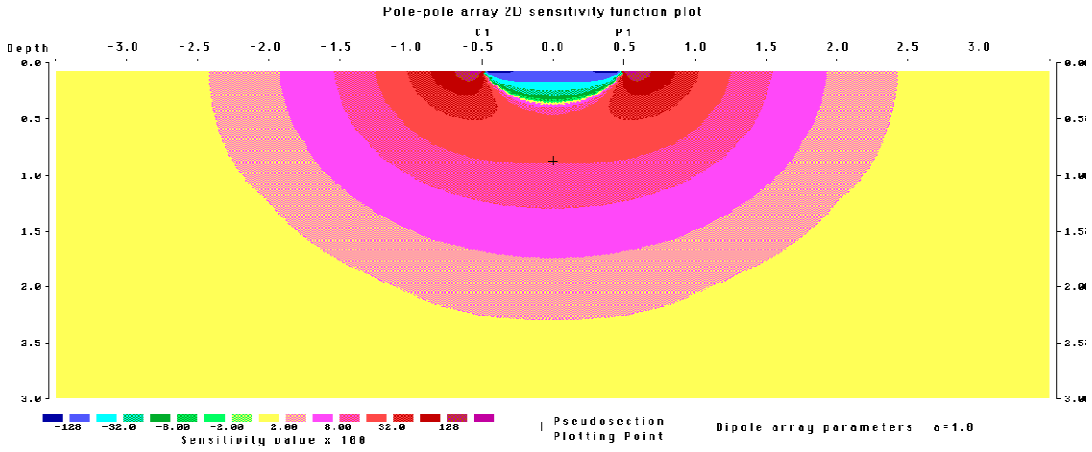

Figure 2.17 Sensitivity plot for Pole-pole Array (Loke M. H., 1999)

2.3.4.5 Pole Dipole Method

The pole-dipole array is an asymmetrical array. In some cases the model obtained after inversion can be influenced by the asymmetry in the measured apparent resistivity values. The effect of the asymmetry can be eliminated by repeating the measurements by arranging the electrodes in the reverse order. With the combination of “forward” and “reverse” pole-pole arrays, any bias in the model caused by the asymmetrical nature of the array can be eliminated. The signal strength of pole-dipole array is significantly higher compared to dipole-dipole array. The pole dipole array is not as sensitive as pole-pole array to telluric noise. This array has relatively good horizontal coverage to determine resistivity which makes it an attractive array for multi-electrode resistivity meter system with a relatively small number of nodes. However, The signal strength is lower compared to the Wenner and Wenner-Schlumberger arrays but higher than dipole-dipole arrays.

2.3.5 Data Acquisition

Single channel instruments required electrode to be reconfigured after each measurements. This methodology is time consuming and laborious. Newer equipment are equipped with multiple channels that includes multiple electrodes where measurements are taken through each channel. SuperSting R8 resistivity meter produced by Advanced Geosciences, Incorporated, is equipped with eight channels. Therefore for each current injection, the system utilized nine electrodes to collect eight different potential difference measurements (Advanced Geosciences, Incorporated 2006). The variation of data measurement of single channel and multichannel system is presented in Figure 2.18.

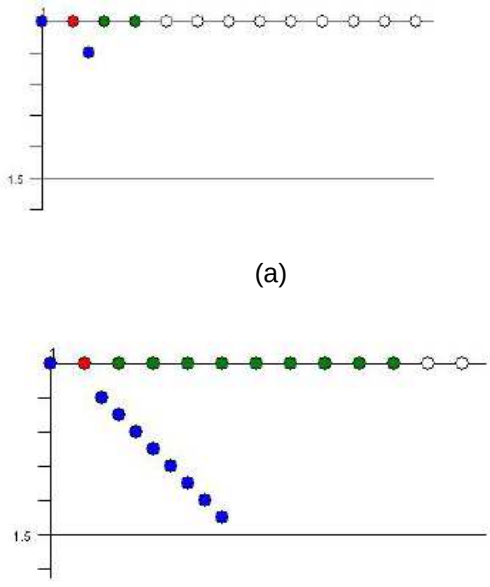

(a)

(b)

Figure 2.18 a. Single channel Instrument (Supersting R1/IP) b. 8-channel Instrument (Supersting R8/IP)

Multiple channel equipment has to receive instruction on the proper triggering sequence of electrodes. This information can be programmed with manual entry or uploaded coded command file. The sequencing information considers the array style, information pertaining to the electrode locations/electrode address during each measuring sequence.

There are no theoretical limits to the depth of penetration. However, for tomography applications, practitioners can greatly assume that the depth of penetration is approximately 15 to 25 percent. The electrode spacing should not be greater than twice the size of the object or feature to be imaged. The design of the survey (i.e. survey run length, electrode spacing, and array type) directly impacts the depth of penetration and resolution (Advanced Geosciences Incorporated 2006).

For the continuous profiling, roll along survey technique can be utilized to continuous profiling of the subsurface along a common survey line. Figure 2.19 presents both two and three dimensional roll along patterns. As shown, a segment of electrodes is detached from the original survey line and relocated to the end of the cable system, effectively advancing the survey along the desired imaging path. As the entire line will not be advanced, not all the reading will be new reading. In Figure 2.19 (a) the overlapping triangular patterns represent the respective field data points or psuedo-section generated during each survey. Based on the instrument and survey design, these readings may either be repeated or disregarded after acknowledging that measurement of the same area is already made. Using multiple cables, the amount of data overlap is reduced and more of the survey can be performed with fewer movements. However, decrease in data overlap will increase the void left below the two overlapping pseudo-sections as presented in Figure 2.19 (a) (Advanced Geosciences Incorporated, 2006).

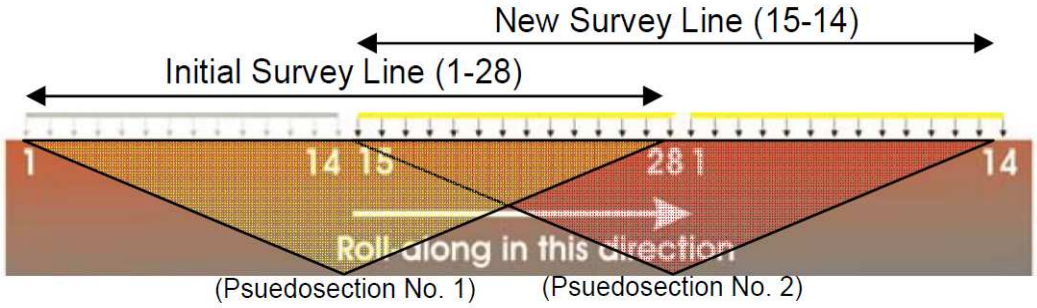

(a)

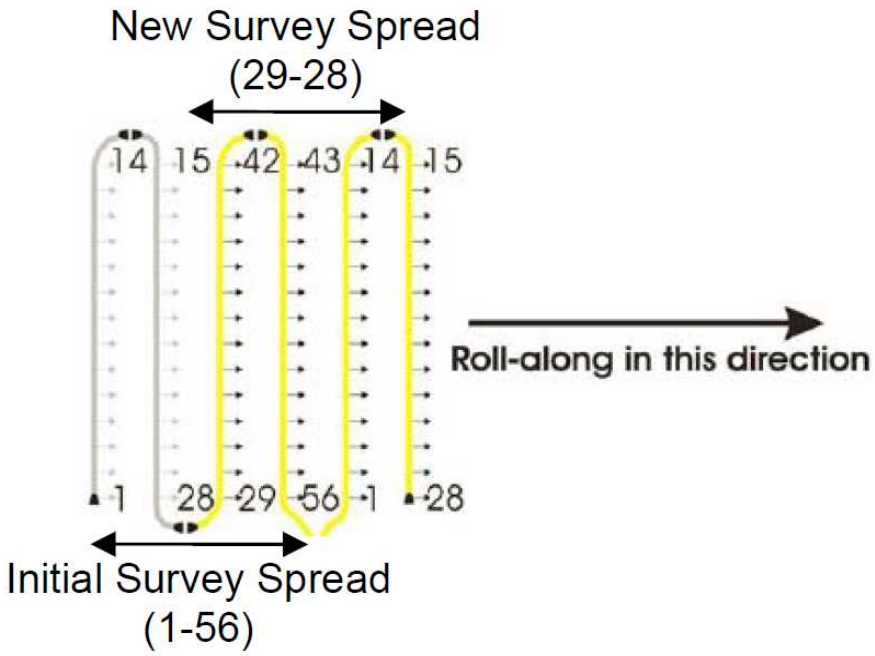

(b)

Figure 2.19 Example of a Roll-Along for (a) Two-Dimensional Survey (b) Three-Dimensional Survey (Advanced Geosciences, Incorporated 2006)

2.3.6 Data Interpretation

Field investigation results of resistivity imaging are converted to a visual representation for analysis. The apparent resistivity is calculated from the geometric factor that depends on the spacing of current and potential electrodes, potential difference and injected current. Induced current and respective potential difference from field measurement, with known array type, the

geometric factor and apparent resistivity can be calculated. The mapping of apparent resistivity values creates a profile which is known as pseudo-section (Hubbard J. L. 2009). Psuedo-sections provide a crude representation of the environment surveyed. Apparent resistivity does not provide the true resistivity and shapes of the anomalies. The apparent resistivity plots in a pseudo-section distort the real subsurface model picture and are closely dependent on the type of electrode array configuration (Samouëlian et al., 2004). However, apparent resistivity can be used to estimate true subsurface condition. Apparent resistivity pseudo-section provides necessary data to complete an iterative inversion process. The purpose of the inversion is to produce a representation earth model pseudo-section. During the inversion process, iteration will be done until the modeled pseudo-section approaches convergence with the measured pseudo-section. A generalized flow chart to complete the inversion process is presented in Figure 2.20. The convergence criterion is usually predetermined tolerance for calculated error between the measured and modeled resistivity. The inversion process is best performed using numerical analysis software due to the quantity of data involved and iterative processes. Software packages RES2DINV, RES3DINV and Earth Imager 1D, 2D, and 3D are examples of products available for inversion processing and inversion (Hubbard J. L. 2009).

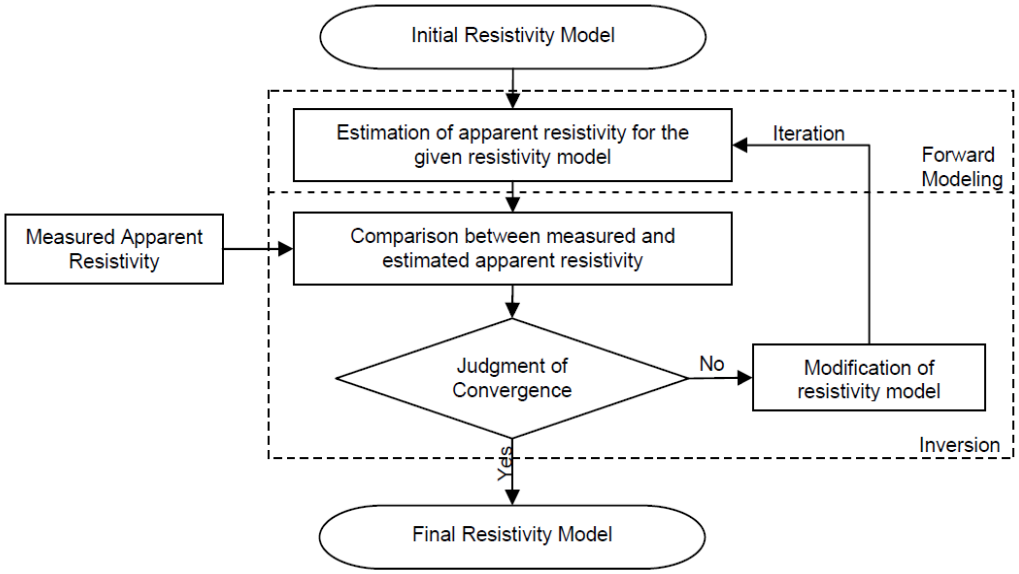

Figure 2.20 Flow Chart of Resistivity Inversion process (Hubbard J. L. 2009).

CHAPTER 3

SITE SELECTION & TEST METHODOLOGY

3.1 Introduction

Determination of unknown bridge foundation is an important issue for the state Department of Transportation's agencies. During this study three bridge foundations were selected to investigate the unknown foundation depth. The bridges are owned by Texas Department of Transportation (TxDOT). The objective of this study is to evaluate the effectiveness of resistivity imaging to determine unknown foundation depth. To meet this objective, 2D resistivity imaging was performed in North Texas region as a part of research project funded by TxDOT. The Bridge sites are: (1) Chamber Creek on FM 916, Grandview (2) Bridge site over Division Street, Arlington and (3) Mountain Creek on FM 2738, Fort Worth, Texas. The site locations are presented in Table 3.1

Table 3.1 Site Location and Foundation Type of Investigated Bridges

Site ID	Site Location	Type of Foundation
Site 1	Chamber Creek on FM 916, Grandview, Texas	Driven steel H-pile
Site 2	Division Street, Arlington, Texas	Drill Shaft
Site 3	Mountain Creek on FM 2738, Fort Worth, Texas	Driven Steel H pile foundation

The bridge sites at Chamber Creek on FM 916 and Mountain Creek on FM 2738 have driven steel H-pile as foundation. The other bridge site over Division Street at Arlington is supported by Drill shaft. Resistivity Imaging was performed by using multichannel High Resolution Resistivity equipment (Model: SuperSting R8/IP). This system includes 56 electrodes with 20 ft of maximum electrode spacing. The penetration depth from this system varies depending on average soil resistivity and the number of electrodes in a single layout. Besides resistivity imaging, Parallel Seismic and Sonic Echo test were also performed in one bridge site to verify the test results from resistivity imaging. This chapter includes the site background; site Geology and field investigation program which are presented below.

3.2 Site Location

Three Bridge foundations were investigated to determine the unknown foundation depth. The site locations are:

3.2.1 Site-1: Chambers Creek on FM -916

The bridge at Chamber Creek on FM 916 is supported by Driven steel H pile foundation. Part of the below grade sections of steel H-pile foundation have been exposed due to the soil erosion at the east and west side of the bank of the creek. . The piles exposure might reduce the capacity of the piles due to the reduction of skin friction from the exposed length. This bridge is located at the Grandview, Johnson county, Texas which is 2 miles east from IH 35W. The location of the bridge is presented in Figure 3.1. The bridge id no. is 071202001 of TxDOT. The site condition under the bridge is presented in Figure 3.2.

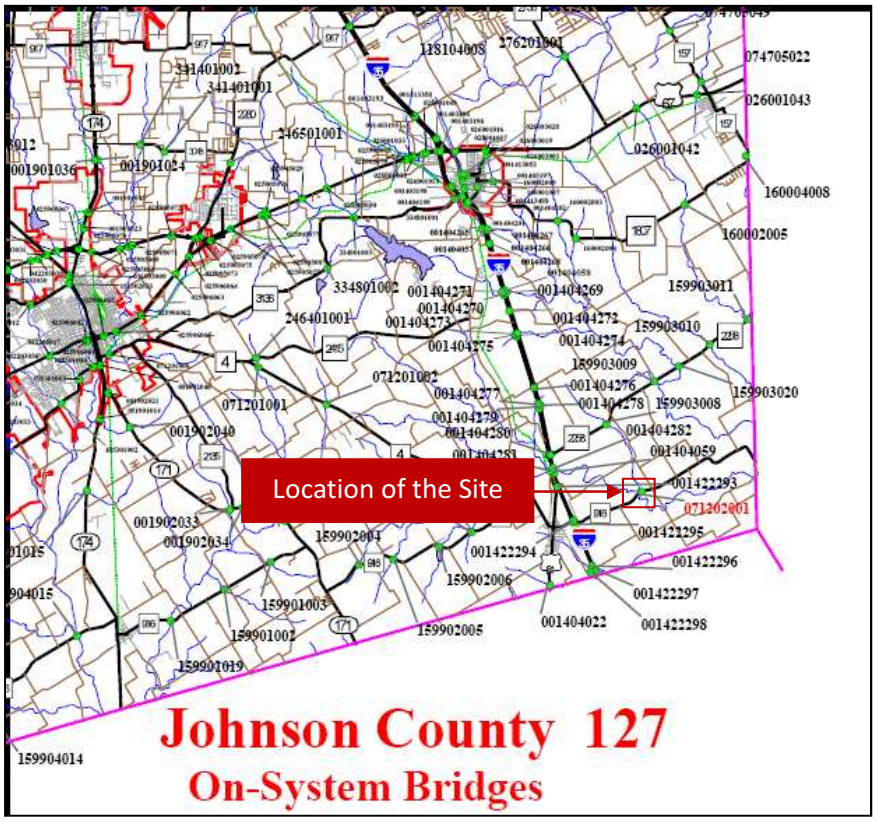

Figure 3.1 Site Location Map (Bridge ID: 071202001)

Figure 3.2 Site Photos of Bridge at FM916 over Chambers Creek

3.2.2 Site-2: Over West Division Street, Arlington.

This bridge site is located on West Division Street, near Green oaks blvd intersection at Arlington, Texas The bridge ID number is 02-220-0008-06-052 of TxDOT. The bridge has 6 (six) span which is supported by Drill Shaft. Figure 3.3 presents the location of the bridge. The site picture of the bridge is presented in Figure 3.4.

Figure 3.3 Location of Bridge sites (02-220-0008-06-052)

Figure 3.4 Site Picture of Bridge sites (02-220-0008-06-052)

3.2.3 Site -3: Mountain Creek on FM 2738

The bridge site is located at Mountain Creek on FM 2738, Fort Worth, Texas. The bridge has two spans supported by 4 (four) driven steel H-pile at the middle. The Site location and site photo of the bridge are presented in Figure 3.5 and Figure 3.6 respectively.

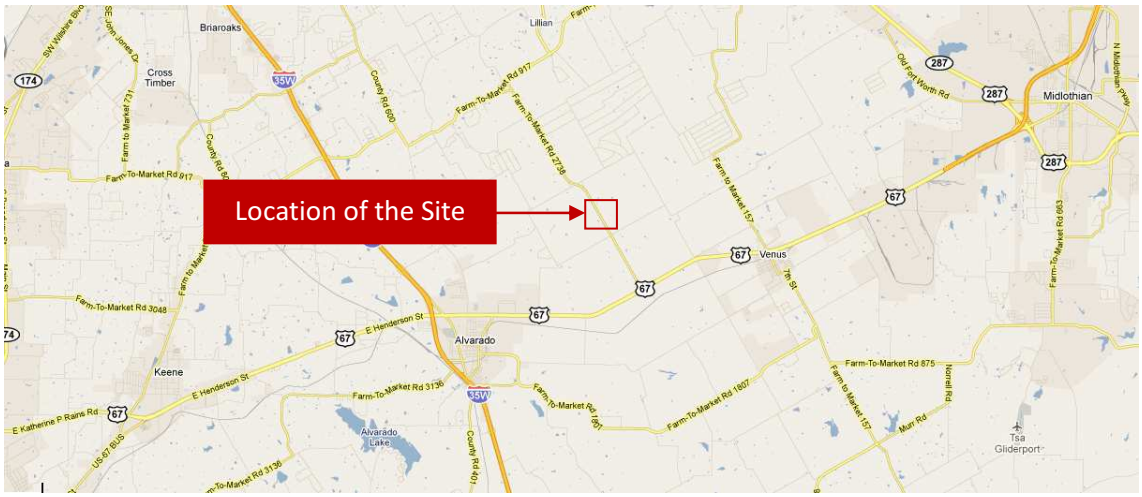

Figure 3.5 Site Location Map (Mountain Creek on FM 2738)

Figure 3.6 Site Photos (Mountain Creek on FM 2738).

3.3 Site Geology

All the 3 (three) bridge site is located at the North of Texas near the Dallas Fort Worth (DFW) Metroplex. The geology of the DFW Metroplex is of tilted sediments of mostly Cretaceous age (en.wikipedia.org). The DFW Metroplex is around 100 km wide in the North South direction. In the west, Fort Worth is built on the Early Cretaceous sediments and Dallas in the east is built on Late Cretaceous sediments. The early Cretaceous sediments deposited over 20 million year interval, having time span between 118 – 98 million years ago (mya), and are responsible for the deposition of the Trinity, Fredsrickberg and Washita groups. These three groups span from slightly west of Weatherford to the east side of Fort Worth.

The Trinity Group is known for the Glen Rose formation which is about 40-200 ft thick, composed of a limestone with alternation units consist of clay, marl and sand. The depositional environment of the Glen Rose was a shallow marine shoreline environment. Cretaceous formations from east of Fort Worth to east of Dallas are part of the Gulfian Series. This west to east formation slowly gets younger in age which range from 97 mya to 65 mya. This series deposited the mid Cretaceous formations in the DFW Metroplex. The Gulfian Series consists of three groups, from oldest to youngest being the Dakota, Colorado and Montana. Woodbine formation is the first in the Gulfian Series lie in the Dakota Group, and formed in a high energy depositional environment. It is mostly composed of large rounded grain quartz sediments. The Woodbine formation thickens to Northward with a range of 175ft to 250 ft. Transgression continued to occur after the deposition of the Woodbine that created the Colorado Group. This Colorado Group first created the Eagle Ford Shale which lies directly beneath west Dallas (en.wikipedia.org).

The Eagle Ford Shale had sea level depths of around 330ft, and occurred around 20-50 km from the shore. The depositional environment of the Eagle Ford Shale had lower energy and slightly anoxic setting at its lower beds. The lower section of the Eagle Ford consists of organic-rich, pyritic, and fossiliferous marine shale. The overall thickness of the Eagle Ford Group is

around 200-300 feet thick. Austin Chalk is around 300 ft to 500 ft thick. This formation occurred around 89 mya to 85 mya. The Austin Chalk formation is consists of recrystalized, fossiliferous, inter bedded chalks and marls. Austin chalk is the well known white rock. Several different layers sits over the Austin chalk are known as Taylor formation. Ozan Marl is the first bed over the Austin Chalk that can be found in city of Richardson and Garland. The Ozan Marl consists of calcareous micaeous clay with increasing silt and sand towards the top. The thickness of Ozan marl is around 500 ft. On the top of the Ozan marl, two thin beds known as the Wolfe city sandstone and Pecan Gap Chalk are found. The top of the Taylor formation has a 300 ft of marls that known as Marlbrook Marl. The last bed of the Cretaceous was deposited over the Taylor formation that are found at the east of Dallas are the Navarro beds. The Geological formations of Texas is presented in Figure 3.7.

The first bridge site at Chambers Creek on FM 916 (Site 1) and the third bridge site at Mountain Creek on FM 2738 (Site 3) is located over the Eagle Ford Shale (www.northtexasfossils.com[a]). The Geology map of these two specific bridge location is presented in Figure 3.8 (a) and Figure 3.8 (c). The Eagle Ford is a bituminous shale with calcareous concretions and large septaria; It has sandstone and sandy limestone in the upper parts and bentonitic in the lower part. The laminated bedding structure and dark color makes the Eagle Ford easy to identify.

The second bridge site is located over Division Street in Arlington. The Bridge site is located over the Quaternary alluvium (Qal) (www.northtexasfossils.com[b]). The Quaternary alluvium is typically a alluvial deposits of sand, gravel, silt, and clay. The location of the bridge site is presented geological map in Figure 3.8 (b).

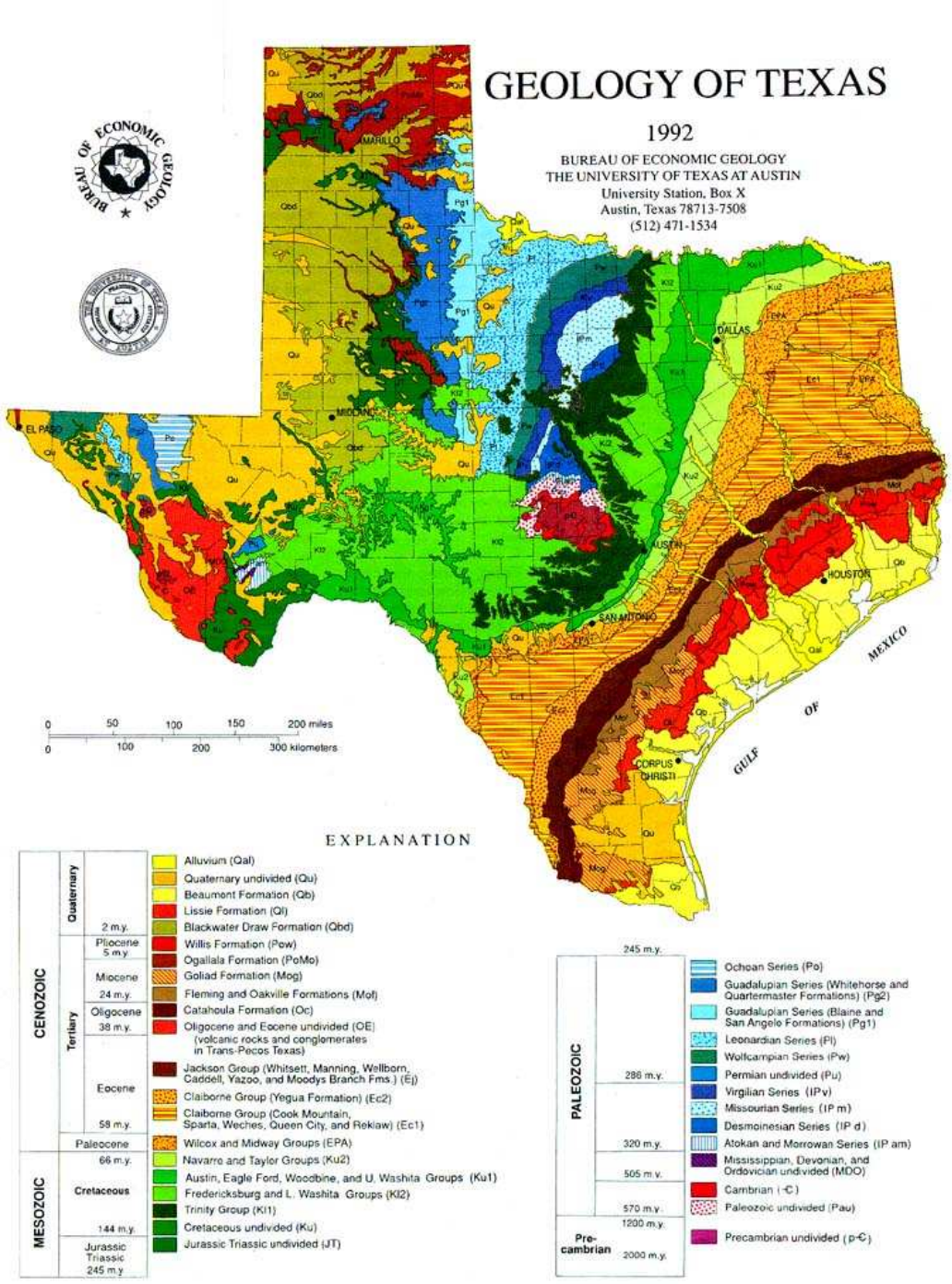

Figure 3.7 The Geology of Texas (http://www.lib.utexas.edu/geo/pics/texas92a.jpgl)

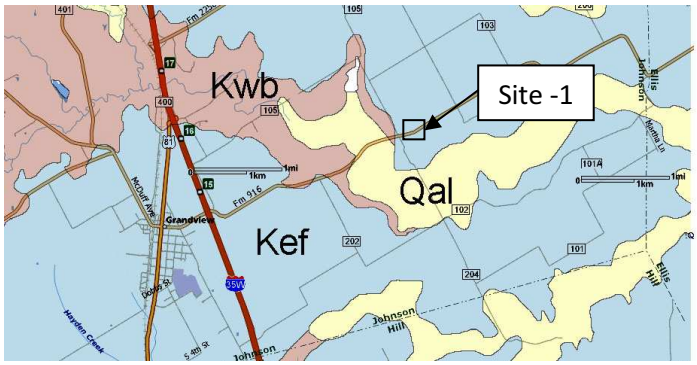

a.

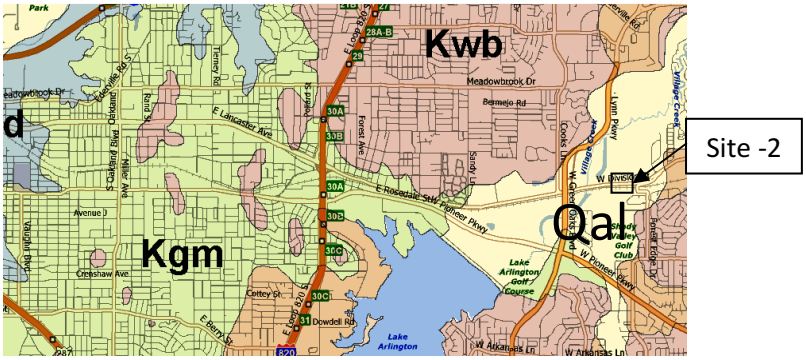

b.

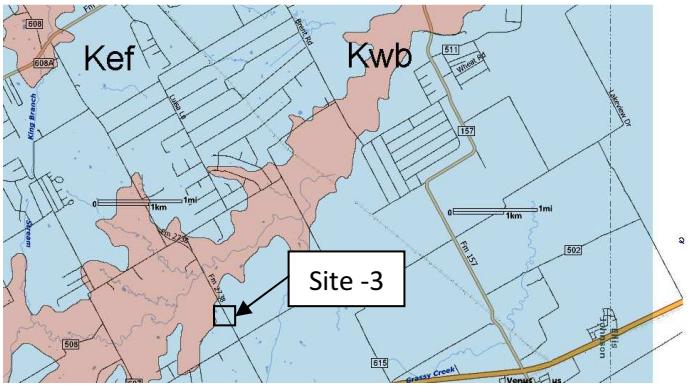

c.

Geological Formations:	
Holocene Period:	**Qal** - Quaternary alluvium
	Qu - Quaternary undivided
Pleistocene Period:	**Qt** - Quaternary terrace deposits
Cretaceous Period:	**Kef** - Eagle Ford
	Kwb - Woodbine

Figure 3.8 Geology map of Specific Site Location a. Chambers Creek at FM 916, b. Division St, Arlington, c . Mountain Creek on FM 2738 (www.northtexasfossils.com)

3.4 Field Investigation Program

Three different bridge foundations were investigated for the purpose of this study. Electrical Resistivity Imaging (RI) was used for determining the depth of all bridge foundations. For one specific site - Site 3, RI, Parallel Seismic and Sonic Echo methods were utilized and their effectiveness in determining unknown bridge foundations were evaluated and compared. The field investigation program conducted during this study is summarized in Table 3.2.

Table 3.2 Summary of Field Investigation Program

Site ID	Location of Bridge Site	Foundation Type	Field Investigation Method
Site 1	Chamber Creek on FM 916, Grandview, Texas	Steel H-Pile	2D RI test
Site 2	Division Street, Arlington, Texas	Drill Shaft	2D RI test
			3D RI test
Site 3	Chamber Creek on FM 916, Grandview, Texas	Steel H-Pile	2D RI test
			Parallel Seismic Test
			Sonic Echo Test

3.4.1 Resistivity Imaging

Resistivity imaging method is carried out to determine surface resistivity of shallow subsurface. SuperSting R8/IP resistivity meter was utilized during the field investigation. SuperSting R8/IP is a multichannel system that includes 8 channels to conduct the survey. The 8 channel system has 8 receivers which is able to take 8 reading for each current injection. Thus, this resistivity imaging instrument is 8 times faster compared to single channel system. This multichannel system includes maximum 56 electrodes. However, 28 electrodes can be utilized to perform resistivity imaging for the site having limited access.

This system allows variable electrodes spacing with maximum 20 ft distance between two adjacent electrodes. In addition, this system includes a SuperSting R8/IP resistivity meter, Switch Box, Electrodes, Cables and 12 Volts battery as power supply. The RI test setup using SuperSting R8/IP resistivity meter is presented in Figure 3.9. Switch Box is used with passive cables and electrodes to form a central switching system. SuperSting R8/IP is available with built in switch box for 28 and 56 electrodes.

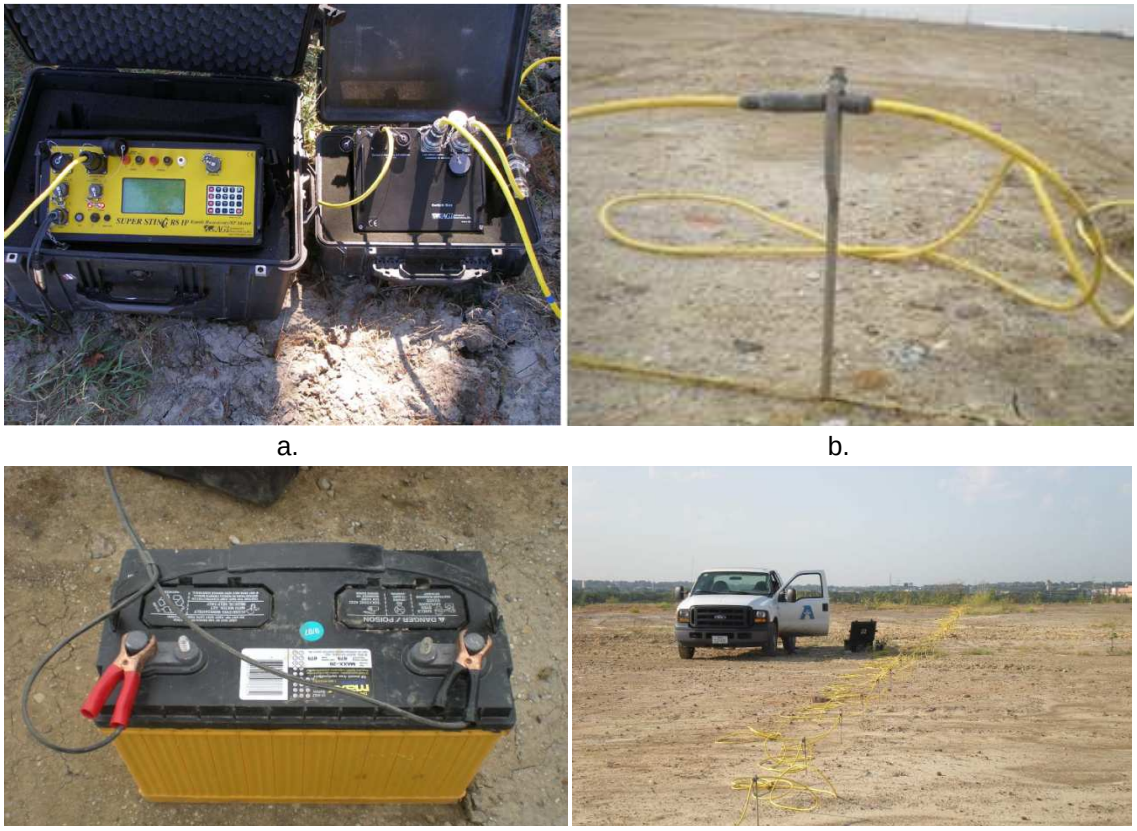

a. b.

c. d.

Figure 3.9 Resistivity Imaging test setup, a. SuperSting R8/IP resistivity meter with Switch Box, b. Electrodes connected with cable, c. 12 Volt Power Supply, d. Resistivity Line

The electrode spacing for resistivity imaging depends on required resolutions for site investigations, size of objects under investigations, and depth of penetration required for the site investigations. Smaller electrode spacing might leads to better resolution, but penetration depth becomes smaller. For the same number of electrodes, larger electrode spacing would lead to

larger depth of penetration. For this current study, both 2D & 3D resistivity imaging were conducted with smaller spacing to get the better resolution.

During RI test, apparent resistivity data were collected and stored in the SuperSting R8/IP meter in a raw form. The raw data were extracted and converted into a suitable form for processing. AGI Administrator software is used to download and convert field data to a readable format for the AGI EarthImager 2D analysis software. From the collected field data, the apparent resistivity can be plotted in the respective pseudo-section. The AGI EarthImager 2D software uses the measured apparent resistivity Pseudo-section to recreate an inverted resistivity section. Inversion is a process that reconstructs the subsurface resistivity distribution from measured apparent resistivity. EarthImager 2D software allows Forward Modeling, Damped Least Squares Inversion, Smooth model Inversion & Robust Inversion (Advanced Geosciences, Incorporated 2006).

During the inversion process, a starting resistivity model is constructed based on either average apparent resistivity, or apparent resistivity distribution. A virtual survey or forward modeling is carried out for a predicted data set over the starting model. The initial root mean square (RMS) error at the zero-th iteration was calculated. The resistivity model is updated using linearized inversion and the model value is adjusted in the finite element mesh. Iteration continues until the model value reached a value where the RMS is within an accepted value. If the level of error is beyond the acceptable limit, the raw data need to be evaluated to determine whether outlier measurement is causing unwanted error in the inverted model. Using misfit histogram generated in the AGI Earth Imager program, corrupting data points can be isolated. This isolation can also be done by manually eliminating data points in the pseudo-section or by suppressing the readings collected from particular electrodes. The iteration process can be stopped when the represented model demonstrates the subsurface condition, within the accepted error tolerances for the survey (Advanced Geosciences Incorporated, 2006).

The RI test performed during field investigation program at three bridge sites to determine unknown foundation depth is presented below.

3.4.1.1 Site-1: Chambers Creek on FM -916

The bridge at Chambers Creek on FM 916 has 5 spans supported by steel driven H-pile. 2D RI test was performed in two sections includes the east side of the bridge and west side of the bride. The layout of the 2D resistivity line is presented in Figure 3.10.

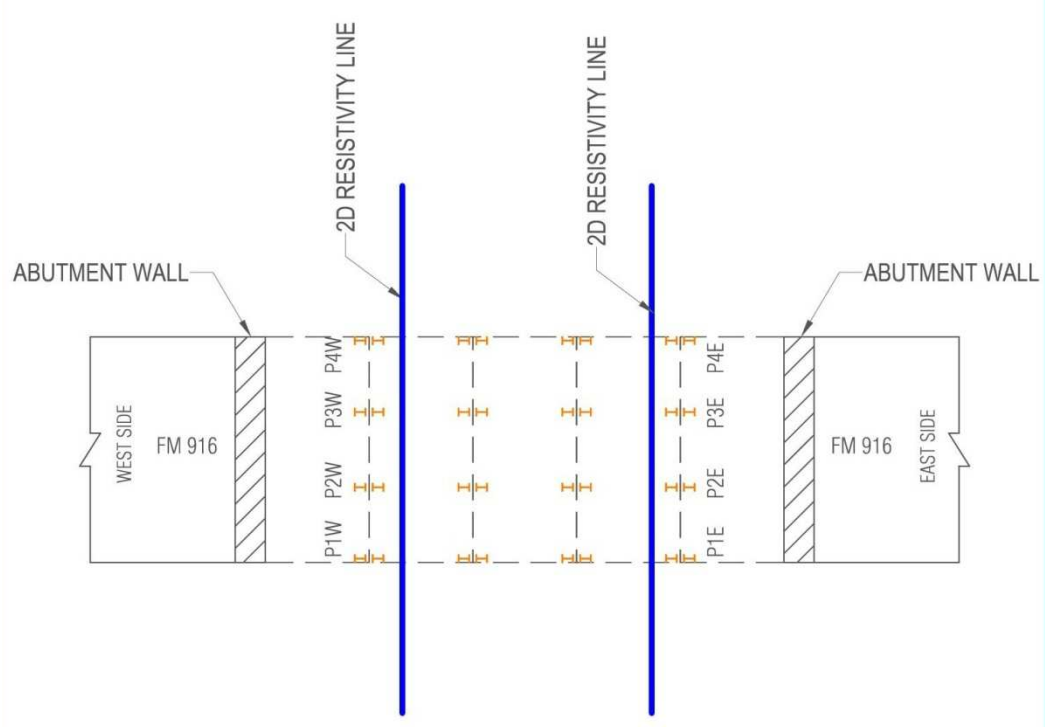

Figure 3.10 Resistivity Layouts of the bridge at Chambers Creek on FM 916

2D RI test under the bridge at Chambers Creek on FM 916 was performed to investigate the unknown foundation depth. The layout of the resistivity line at both east and west side of the bridge is perpendicular to the direction of traffic. The electrode spacing for both line at east and west side was 2 ft. Total 28 of electrodes are used during each test. The total length of the resistivity line was 54 ft. The resistivity imaging field set up for west and east side of the

bridge is presented in Figure 3.11 and Figure 3.12 respectively. Dipole-Dipole array is suitable for field investigation and was used for both of the test. The test data was recorded during the field investigation program and was transferred to a computer for further analysis.

Figure 3.11 Resistivity Imaging Layout on the West side of the bridge

Figure 3.12 Resistivity Imaging Layout on the East side of the bridge

3.4.1.2 Site-2: West Division Street, Arlington

2D and 3D RI test was conducted for the determination of unknown foundation depth at the bridge on West Division Street, Arlington, Texas having TxDOT Bridge ID 02-220-0008-06-052. The bridge had 6 span supported by Drilled Shaft. The layout of both 2D and 3D resistivity line is presented in Figure 3.13.

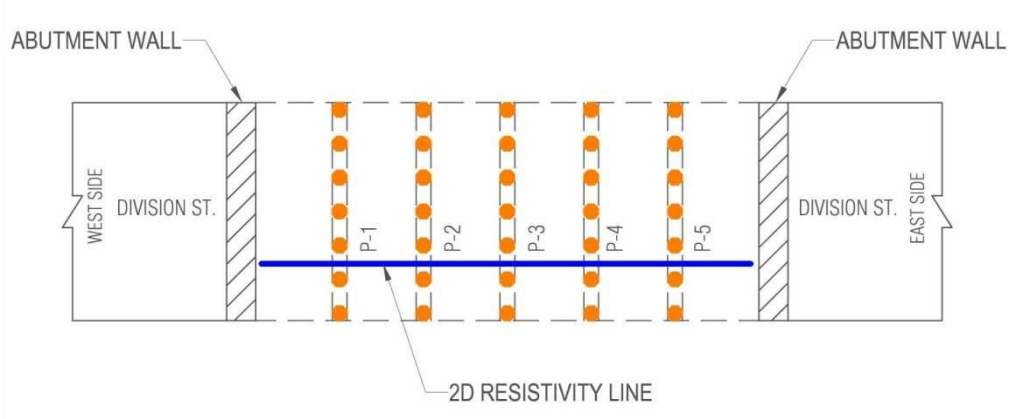

a.

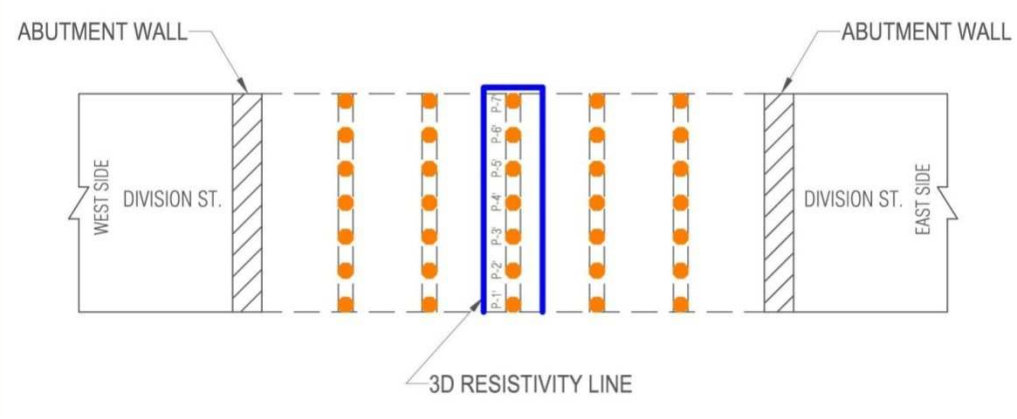

b.

Figure 3.13 Resistivity Imaging Layout for bridge foundation over West Division Street, Arlington, a. 2D Resistivity Line, b. 3D resistivity Line

The 2D resistivity line was parallel to the direction of the traffic where the electrodes were placed at 2 ft spacing. Total 56 of electrodes are used during the test set up. Total length of the resistivity line is 110 ft. The 2D resistivity imaging field set up is presented in Figure 3.14 (a). During this test Dipole-Dipole array was used due to its strong sensitivity. In the resistivity set up the Pile group P1 is located in between electrode 3 and 4, P2 is located in between electrode 16 and 17, P3 is located in between electrode 28 and 29, P4 is located in between electrodes 41 and 42 respectively and P5 is located in between electrode 53 and 54 respectively.

3D RI test was performed at the middle row of the bridge. The electrode spacing for 3D resistivity was 2.5 ft. The field set up of 3D resistivity line is presented in Figure 3.14 (b). The 3D profile was considered with 2 row of electrodes where 28 electrodes are provided in each row. During the Field investigation test, the pile P1' is located beside electrode 4, pile P2' is located in between electrode 6 and 7, pile P3' is located beside electrode 9, pile P4' is located in between electrode 12 and 13, pile P5' is located beside electrode 16, pile P6' is located in between electrode 19 and 20 and pile P7' is located beside the electrode 23 respectively. The test data was recorded during the field investigation program and was transferred to a computer for further analysis.

a.

b.

Figure 3.14 RI test at bridge on Division Street, Arlington, a. 2D resistivity field set up, b. 3D resistivity field set up.

3.4.1.3 Site -3: Mountain Creek on FM 2738

The resistivity imaging was conducted at the bridge on FM 2738 at Mountain Creek to determine the sub surface resistivity profile and to investigate the unknown foundation depth. 2D resistivity imaging was conducted across the direction of traffic under the Bridge at Mountain Creek. The Layout of the resistivity line is presented in Figure 3.15. Thus Dipole-Dipole array is utilized for the field investigation.

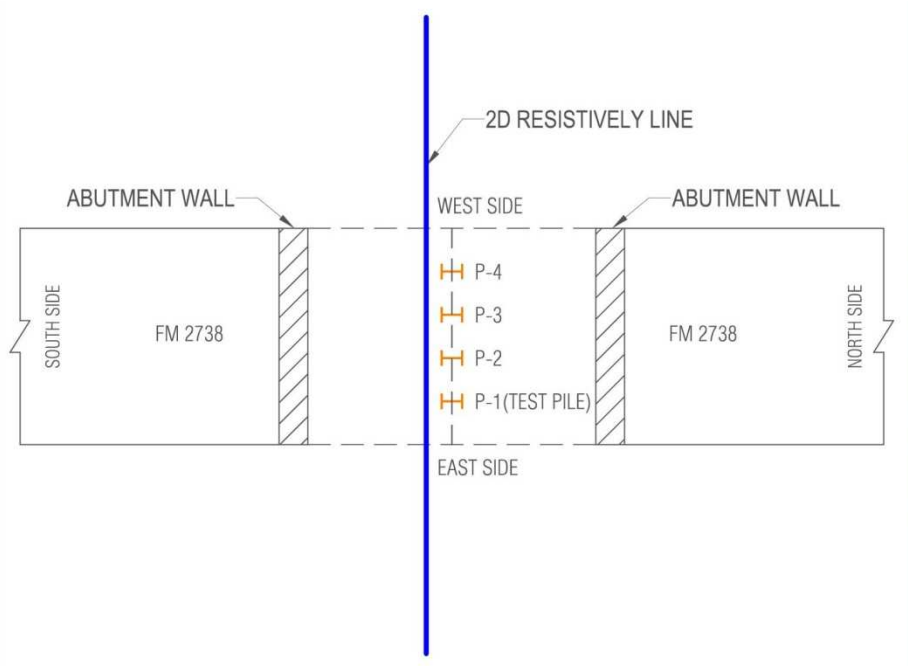

Figure 3.15 Resistivity Layout for Bridge foundation Mountain Creek on FM 2738

The bridge was supported by four steel H-piles (P1, P2, P3 & P4). Total 56 electrodes are utilized during the operational set up of the resistivity imaging. The spacing between the electrodes is 2 ft for all test configurations. The total length of the line of resistivity imaging is 110 ft. Figure 3.16 presents the resistivity field set up.

Figure 3.16 Resistivity Set up for Mountain Creek on FM 2738

In the resistivity set up, the pile P4 was between electrode 27 and 28, pile P3 is between electrode 31 and 32, pile P2 is between electrode 34 and 35 and P4 is between electrodes 37 and 38. The test data was recorded during the field investigation program and was transferred to a computer for further analysis.

The pile foundation depth was also investigated by using Parallel Seismic method and Sonic Echo method, the methods are discussed in next section.

3.4.2 Parallel Seismic Method

The parallel seismic (PS) method is based on the principle that an impact to the exposed structure generates wave energy that travels down the foundation. This wave energy can be tracked with receivers in a nearby boring parallel to the structure. Based on the energy dissipation and velocity, the unknown foundation depth can be determined (Olson et al., 1998). For parallel seismic testing, a short duration impact with high energy is required which needs to be identified by the receiver (Finno et al. 1997). The PS method involves impacting the side or top of exposed bridge substructure with an instrumented hammer to generate wave energy. The impact to generate the wave energy can either be vertical or horizontal. The test can also be performed using a non-instrumented hammer where accelerometer needs to be mounted at

nearby impacted area (Sack & Olson, 2009). The generated wave energy travels down the foundation and is refracted to the adjacent soil throughout the foundation. The refracted wave arrival is tracked by using hydrophone or geophone receiver. Hydrophone is suspended in a water-filled cased bore hole. A hydrophone receiver is sensitive to pressure changes in the water filled tube. The cased boring is required to be placed within 3 to 5 feet of the foundation edge. The cased boring placed within 3 to 5 feet of the foundation edge, gives more accurate results than any other orientation. With increase in distance between the casing and foundation, the refracted wave energy gets weaken and the signal received by the hydrophone may have noise. However, the bore hole can be placed as much as 15 feet distance from foundation edge depending on the soil condition. The cased bore hole need to be extended at least 10 feet deeper than the anticipated depth of the foundation.

During this study, the PS test was performed only in Bridge site on FM 2738 at Mountain Creek. Pile P1 as presented in Figure 3.15 is tested using PS method to cross check the field investigation result from RI test. Soil test borings were conducted beside pile P1 which was then utilized to install casing pipe to facilitate the PS test. Two casing pipe with different backfill materials were installed to perform PS test. The effect of different backfill materials were also investigated during this study. The layout and site photo of the casing pipe are presented in Figure 3.17 (a) and Figure 3.17 (b). Before installation, both the PVC pipes were capped at the bottom. Cement-bentonite was used for Casing 1 as backfill material during installation. On the other hand, Casing 2 was backfilled with sand after installation.

The casing was filled with water before lowering the hydrophone. The test pile was impacted at its exposed area with an instrumented 3 lb impulse hammer, and subsequently hydrophone was raised in the bore hole. The data was collected at every 1 feet interval. The collected data were analyzed using a software package IX Foundation (version 1.02). The PS test photo is presented in Figure 3.17.

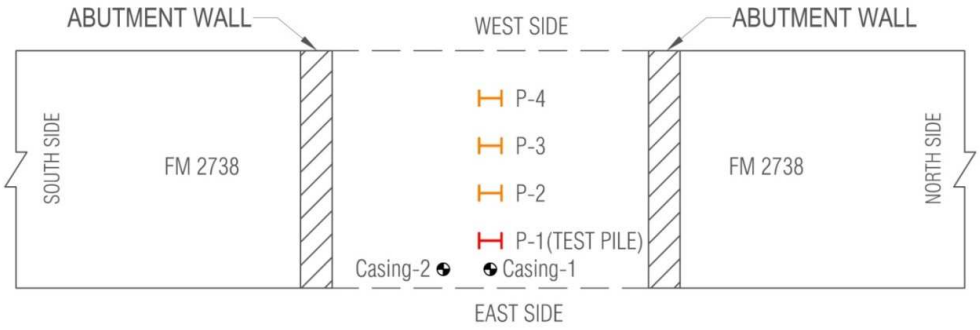

a.

b.

c. d.

Figure 3.17 Parallel Seismic Test a. Layout of Casing Pipe b. Installed Casing Pipe, c. Hydrophone adjustment at every 1 feet interval (d) data acquisition

3.4.3 Sonic Echo Method

The Sonic Echo (SE) test is a low strain dynamic test where the pile is impacted from the top of its surface. This test is also performed to determine the depth and integrity of the structure. SE method is based on the principle that stress wave reflects from significant change in stiffness (Olson et al., 1998). SE test method involves impacting the top of deep foundation with an impulse hammer to generate a downward traveling compressional wave. However, this test cannot be performed impacting the foundation from its side that generate shear wave. The generated compressional wave energy due to vertical hammer impact travels through the foundation and reflects back to the surface when it faces changes in stiffness, cross-sectional area and density. The arrival of the reflected compressional wave energy is sensed by a receiver (accelerometer or vertical geophone). In the SE test, the data is analyzed in time domain.

Sonic Echo test was performed only on the bridge at Mountain Creek over FM 2738 during this study. The same pile tested for Parallel Seismic method was tested for Sonic Echo method. The steel H-section test pile was impacted with instrumented 3lb impulse hammer. SE method requires the foundation top to be impacted at the top of the foundation. However, there was no accessibility to the top of the foundation. Therefore, a triaxial accelerometer was utilized as a receiver attached with the H-pile. SE test photos are presented in Figure 3.18.

Figure 3.18 Field Performance of Parallel Seismic Method

CHAPTER 4

RESULTS & DISCUSSION

4.1 Field Investigation Results

The objective of this study was to determine the unknown bridge foundation depth using resistivity imaging. 2D and 3D Resistivity Imaging (RI) was utilized to fulfill this objective. Three bridges owned by TxDOT at North Texas region were investigated. Parallel Seismic and Sonic Echo method were also utilized to investigate the unknown foundation depth besides the RI method in one bridge site. The field investigation test results are presented below:

4.1.1 Investigation Site-1: Chambers Creek on FM -916

2D resistivity imaging was performed at this site to determine the unknown foundation depth. The test was performed at both East and West side of the bridge. The bridge was supported by steel H-pile foundation. Based on the field investigation, the inverted resistivity pseudo-section for the east side and west side of the bridge is presented in Figure 4.1 and Figure 4.2 respectively. The foundation soil was clayed soil. During the resistivity imaging the top ground surface was observed wet and soft as presented in Figure 4.3. Due to driving of the pile at the clayed soil, disturbance of the soil may not much below the pile foundation. However, disturbance may occur at the adjacent soil beside the pile. In Figure 4.1 and 4.2 a low resistivity zone (blue area) was observed which is representative of natural soils with high moisture zone.

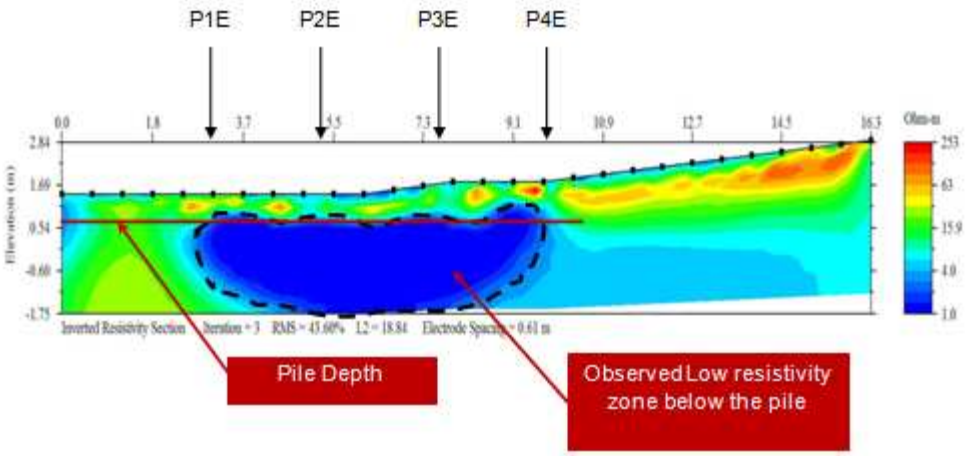

Figure 4.1 Resistivity Profile of Bridge at FM916 over Chambers Creek (East Side)

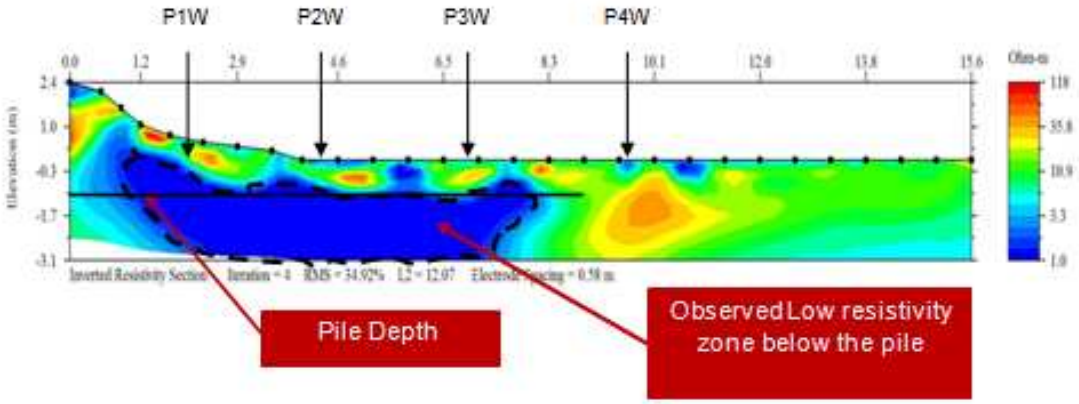

Figure 4.2 Resistivity Profile of Bridge at Chambers Creek overFM916 (West Side)

Figure 4.3 Wet ground surface during RI test.

The location of the pile (P1 to P4) is presented also in Figure 4.1 and Figure 4.2. In the figures, a low resistivity zone was observed just below the foundation. The variations of resistivity with depth under each pile foundation are presented in Figure 4.4 & Figure 4.5.

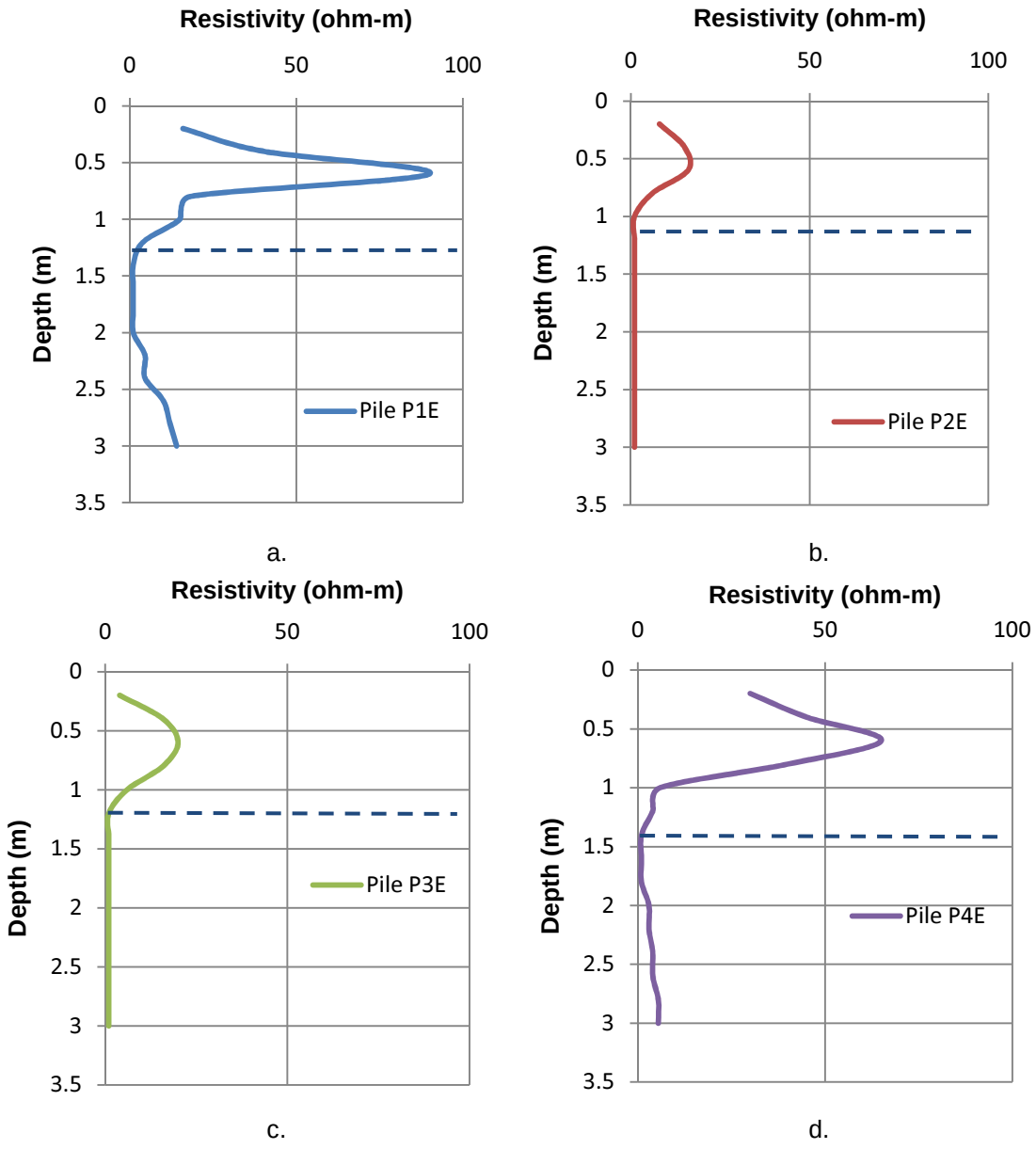

Figure 4.4 Variation of Resistivity for Chambers Creek over FM 916 (East Side)
a. Pile P1E, b. Pile P2E, c. Pile P3E & d. Pile P4E

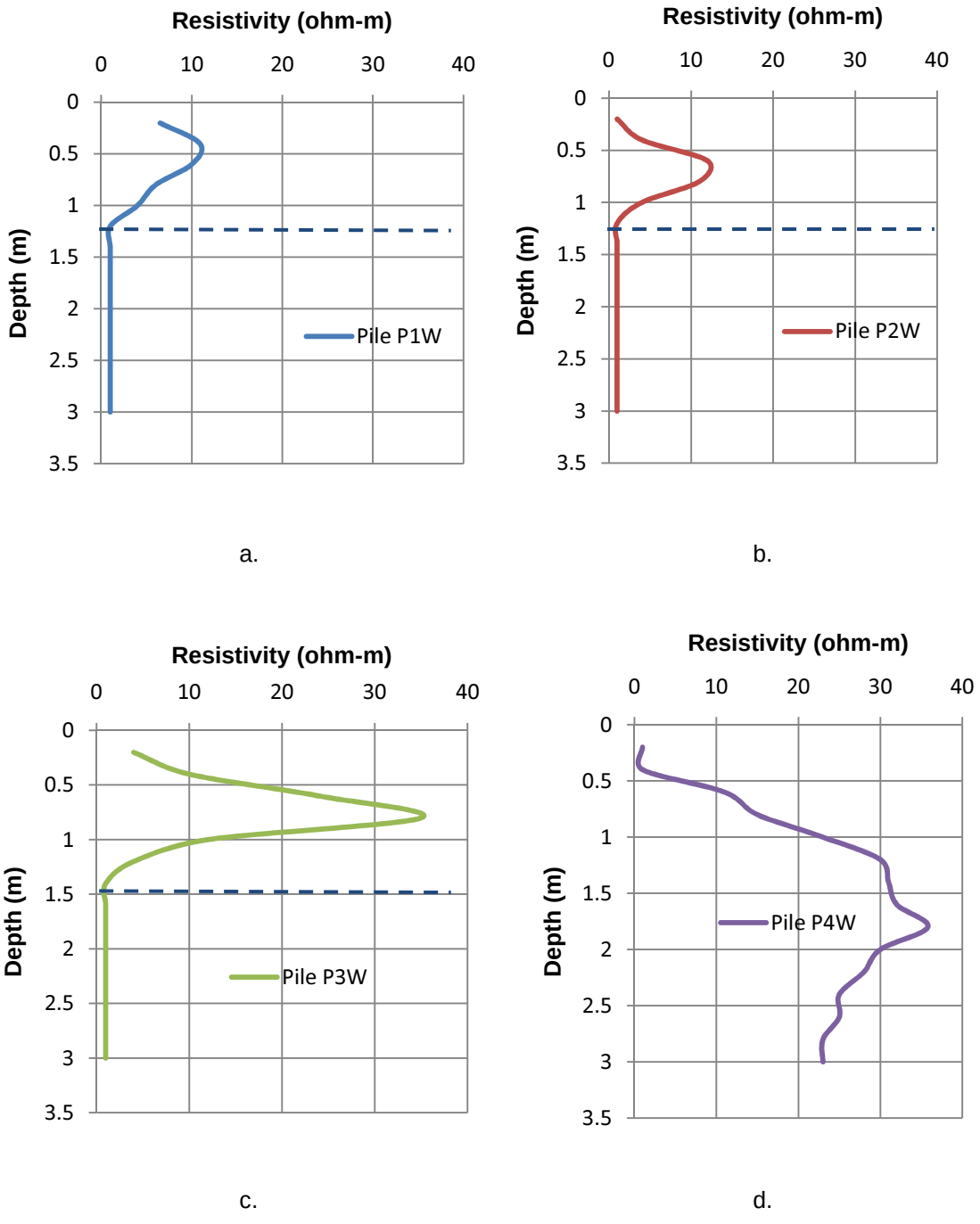

Figure 4.5 Variation of Resistivity for Chambers Creek over FM 916 (West Side)
a. Pile P1W, b. Pile P2W, c. Pile P3W & d. Pile P4W

Based on the results presented in Figure 4.4 and 4.5, a sharp drop of resistivity was observed. Higher resistance was observed around the pile, due to presence of different materials other than soil. This variation in the resistivity can be considered as a foundation depth. For pile P1E to P4E as presented in Figure 4.4 (a) to Figure 4.4 (d), a sharp drop in the resistivity was observed at depth of 1.25 m. Thus the pile depth is considered at the sharp drop of the resistivity and depth of the pile from Figure 4.4 is 1.25 m or 4 ft.

For pile P1W to P3W from Figure 4.5(a) to Figure 4.5(c), a sharp drop of resistivity was also observed at depth 1.25 m similar to the Figure 4.4. The depth of the pile is considered as 1.25 m from the plot below the ground level. However for pile P4W, no significant variation of resistivity was observed from Figure 4.5 (d) to identify the disturbed zone. Thus no depth of the foundation can be determined for pile P4W at the west side of the bridge.

4.1.2 Site-2: West Division Street, Arlington.

The bridge at West Division Street, Arlington is supported by Drill Shaft. The bridge has 6 (six) spans. Both 2D and 3D resistivity imaging were conducted in this test site. The 2D resistivity imaging line was performed along the direction of traffic. Total 56 electrodes were used during this investigation with 2 ft inter electrode spacing. The 2D resistivity imaging results are presented in Figure 4.6.

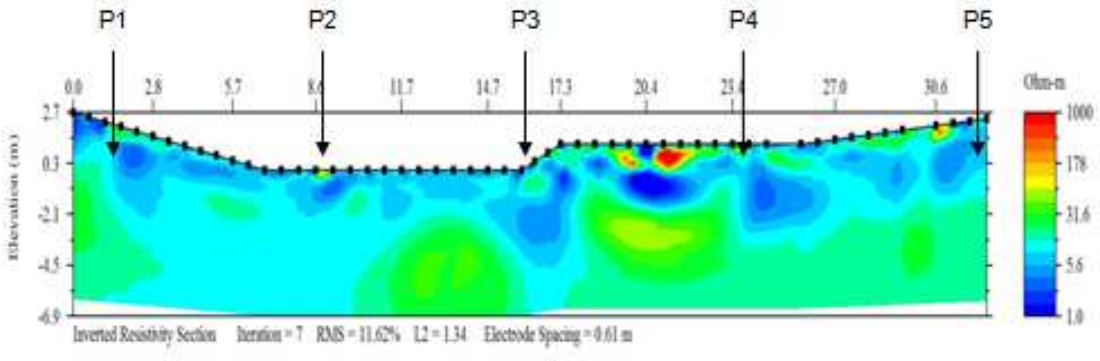

Figure 4.6 2D Resistivity Imaging of West Division Street, Arlington

The location of the Drill Shaft (P1 to P5) in the resistivity imaging profile is also presented in Figure 4.6. The resistivity variation below each pile is presented in Figure 4.7.

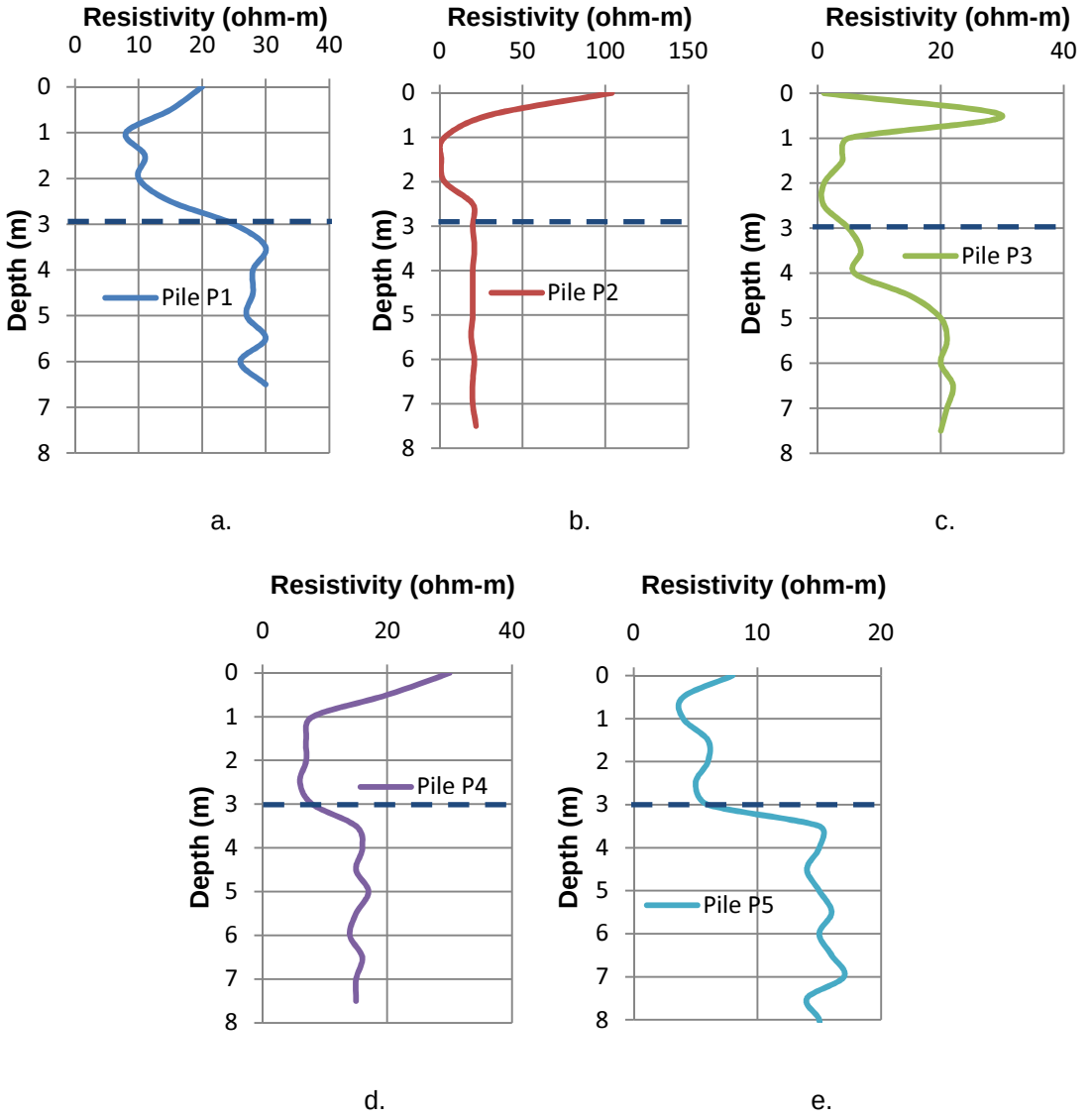

Figure 4.7 Variation of Resistivity bridge at Division St. Arlington a. Pile P1, b. Pile P2, c. Pile P3, d. Pile P4, e. Pile P5

From the variation of resistivity plot as presented in Figure 4.7 (a) to Figure 4.7 (e), a drop of resistivity is observed at a depth starts from 1 m and extents up to 2 m to 4 m. The average variation of resistivity may be considered at 3 m as the depth of the drill shaft.

A 3D resistivity imaging was also conducted below the bridge during the investigation program. The 3D resistivity imaging profile is presented in Figure 4.8.

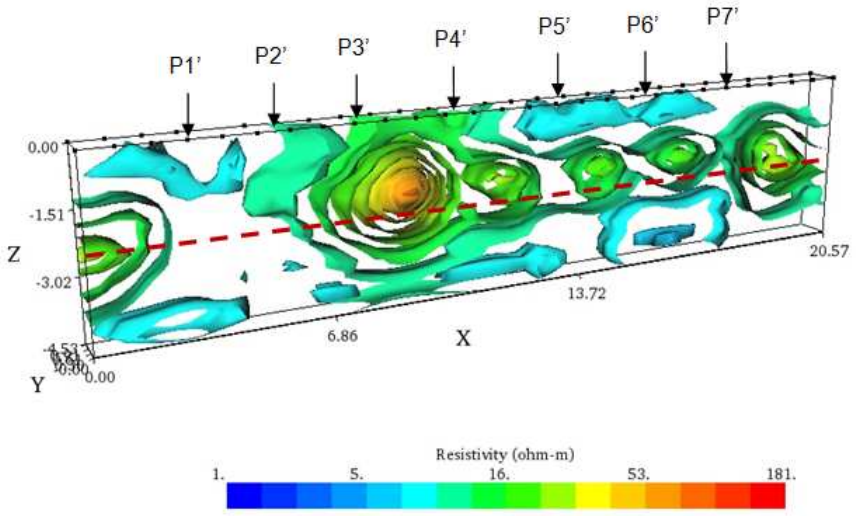

a.

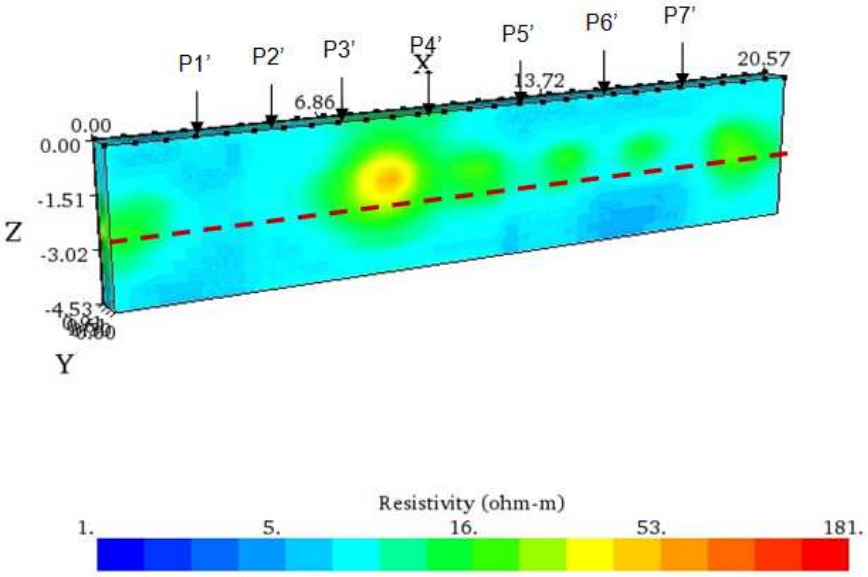

b.

Figure 4.8 3D resistivity imaging results a. 3D contour plot b. Inverted resistivity image

From 3D resistivity imaging results as presented in Figure 4.8, a variation of resistivity was observed below the pile points at 3 m depth, which is similar to 2D Resistivity Data.

A 2D and 3D resistivity imaging was performed at a bridge foundation supported by drill shaft located on Division Street, Arlington to determine the unknown depth of the foundation. Both from the 2D and 3D resistivity profile, the pile depth may be considered as 3 m. During the 2D resistivity profile, the length of the resistivity line was 110 ft. The penetration depth observed during the 2D resistivity imaging was observed 7.2 m or 23.6 ft. During the 3D resistivity imaging, the length of line was 67.5 ft and the penetration depth observed from the test results is around 15 ft. However, if the pile depth is more than 24 ft, the results may be misleading conclusion. The site was not accessible to perform a 2D resistivity investigation across the direction of traffic at a larger line to attain higher penetration depth. Thus site accessibility may become a short coming to determine the unknown foundation depth using resistivity imaging.

4.1.3 Site -3: Mountain Creek on FM 2738

A 2D resistivity imaging was conducted in the bridge site at Mountain Creek on FM 2738 to determine the unknown foundation depth. The bridge are supported with 4 (four) steel H-pile foundation. Total 56 electrodes are utilized with 2 ft spacing during the test set up. The inverted resistivity pseudo-section is presented in Figure 4.9. The resistivity distribution below the pile P1 to P4 is presented in Figure 4.10.

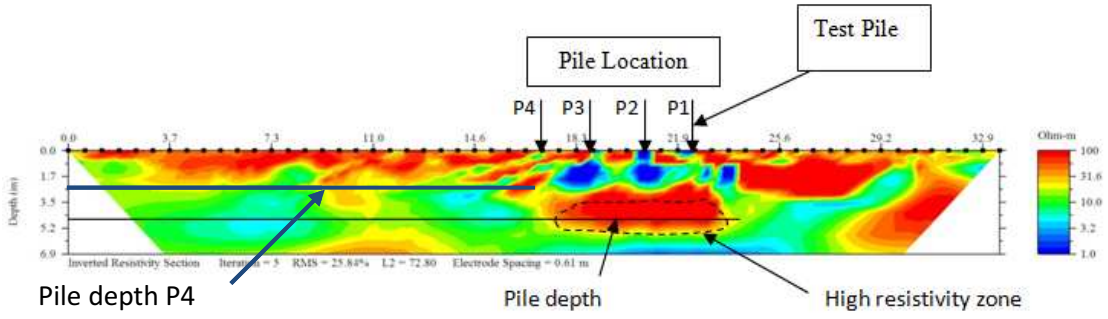

Figure 4.9 Resistivity imaging results on bridge foundation at Mountain Creek over FM 2738.

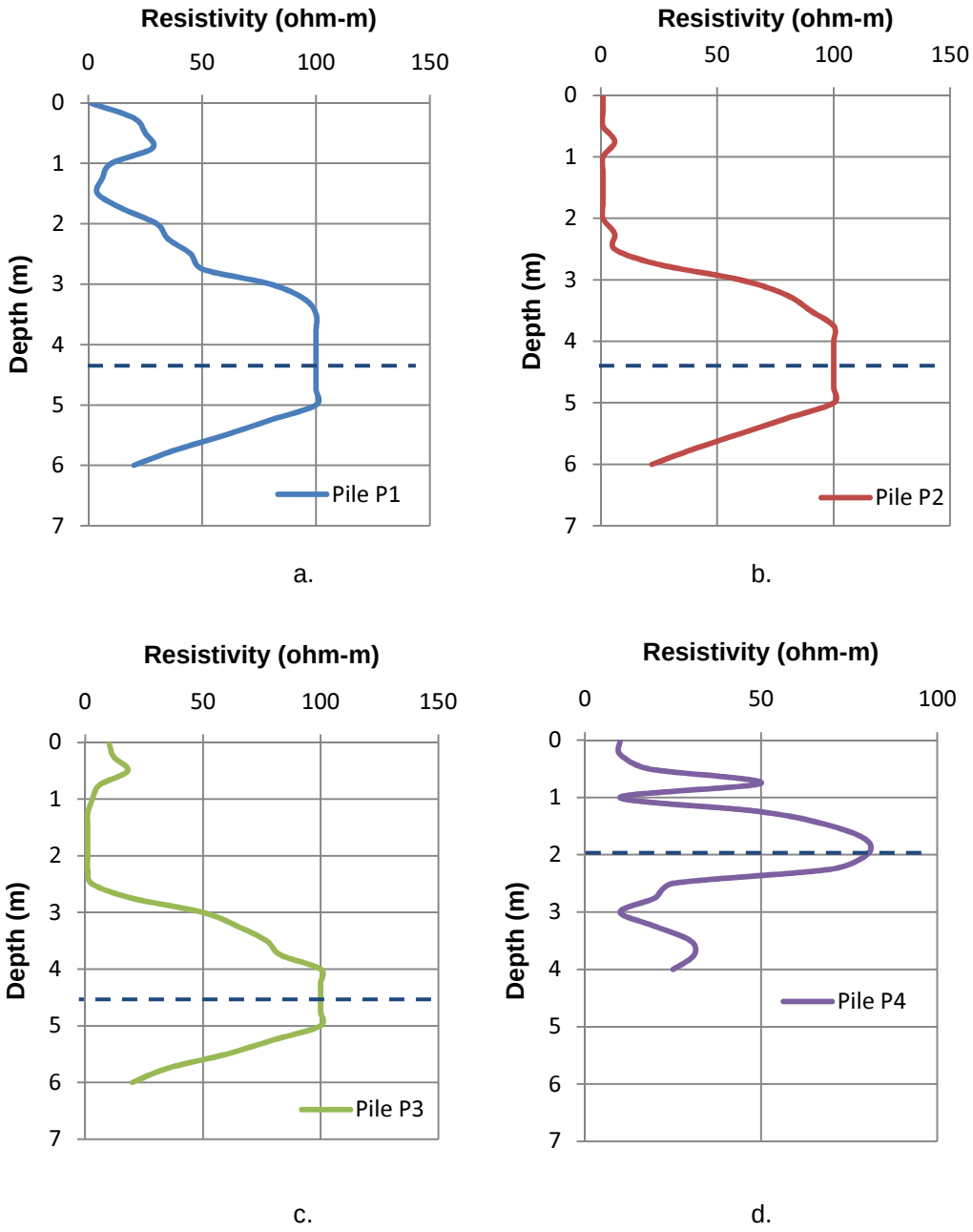

Figure 4.10 Variation of Resistivity under bridge foundation at Mountain Creek at FM2738
a. Pile P1, b. Pile P2 c. Pile P3, d. Pile P4

The bridge was located at Fort Worth, Texas. Based on Site investigation, the top 7 ft of foundation soil was determined as High plastic clay; Disintegrated Eagle Ford Shale was found immediately below the clayey soil followed by stiff Eagle Ford Shale.

During the installation of driven pile in this bridge site, the H-pile is driven into the foundation soil. As a result, a disturbed zone or compacted soil zone is expected to be present immediately below the pile tip. The extent of disturbed zone may be located ± 2D (D is diameter of Pile) from the bottom of pile. During resistivity imaging, current goes through the disturbed zone and the resistance of the compacted or disturbed zone is expected to be different from the natural or undisturbed soil zone. Based on the resistivity results as presented in Figure 4.9, a zone of high resistivity materials were observed and the unknown foundation depths were determined from there. From the variation of resistivity as presented in Figure 4.10 (a) to Figure 4.10 (c), an increase in resistivity is observed from 3.5 m to 5 m below the pile. Thus, the depth of the H-pile foundation is determined at the average of the high resistivity zone and the pile foundation is determined as 4.35 m or 14.25 feet. From Figure 4.9 and Figure 4.10 (d), it was observed that, high resistivity zone was observed at a foundation depth of 2 m or 6.5 ft below the ground level. Thus the pile length for pile P4 was shorter than the rest of the three piles. From this investigation, it can also be concluded that, 2D resistivity distribution provides information about the pile in a group and variation of depth in between the piles in a group can be determined.

The Pile P1 is also tested using PS and SE method to verify the resistivity imaging results. The PS and SE test results are given below:

4.1.3.1 Parallel Seismic Method

Determination of foundation depth from PS test data depends on breaks in the slope of the lines in a plot of depth versus recorded time, drop in energy amplitude below the bottom of the foundation and diffraction of wave energy at the bottom of the foundation (Dennis and Olson, 2009).

Two bore holes were installed beside the pile P1 of bridge at Mountain Creek over FM 2738 to perform the PS test. The casing 1 & casing 2 were backfilled with cement grout and

sand respectively. The field investigation data are collected and analyzed with a computer software package IX Foundation (Version 1.02). The analyzed result of PS Test is presented in Figure 4.11. Based on test results from Parallel Seismic test, it can be mentioned that the foundation bottom is at the intersection point of the two velocity lines (at the inflection depth).

Figure 4.11 (a) presents the field investigation performed at Casing -1 (Using Cement Grout Backfill) and Figure 4.11 (b) represents the PS test results performed at Casing -2 (Using Sand Backfill). The depth of the test pile using PS method performed at Casing-1 was determined as 14.0 ft. On the other hand, PS test performed at Casing-2 (casing backfilled with sand) was 14.5 ft.

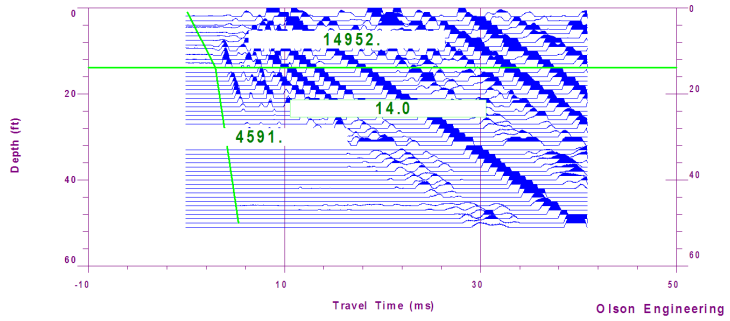

a.

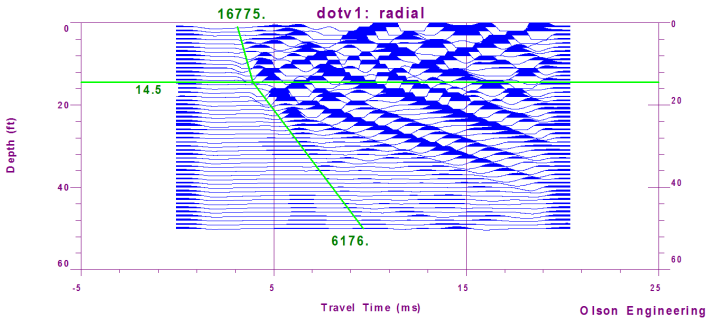

b

Figure 4.11 Parallel Seismic Test Result a. at Casing – 1, b. at Casing - 2

The accuracy of the method depends on the variability of the velocity of the surrounding soil and the spacing between the borehole and the foundation element. Depths are generally determined within 5% accuracy using PS method (Olson et al, 1998).

4.1.3.2 Sonic Echo Method

Sonic Echo test was also performed at the pile P1 of bridge at Mountain Creek over FM 2738. During the SE test no significant trace of the reflection was observed. The weak strength frequency is repeatedly amplified to detect bottom echo and with time domain analysis the H-pile depth was determined as 30.6 feet from SE test as presented in Figure 4.12. However, with repeating amplification of the signal to identify bottom echo, there is a possibility of noise amplification which may leads to misleading results.

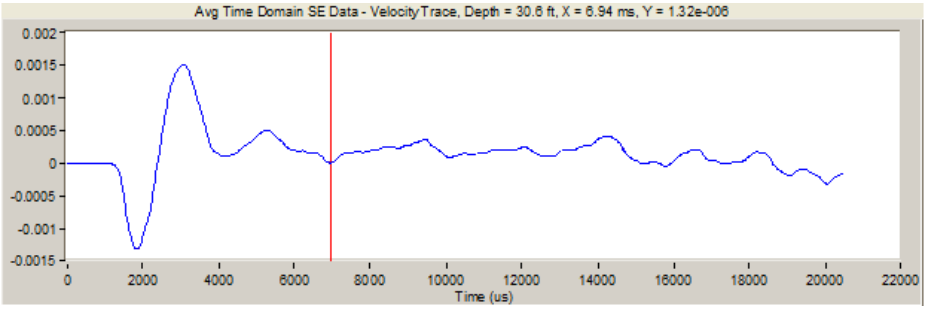

Figure 4.12 Sonic Echo Test Result

When embedded length to diameter ratio for drilled shafts or columnar structures are greater than 20:1 to 30:1 in stiffer soil, there are no significant identifiable bottom echoes due to excessive damping of the compression wave energy. The problem is even worse for steel H-piles which have larger surface area comparing to square or circular pile (Olson et al., 1998). Due to higher surface area of the H-pile, the signal transmits through the soil at higher rate and get damped. Thus, the strength of wave weaken due to higher surface area of the H-pile and so no significant trace of reflected wave was found from SE test.

4.2 Comparison of Field Investigation Results

Resistivity imaging was performed at three sites where as Parallel Seismic and Sonic Echo test was perform at one site to determine the unknown foundation depth. The investigated pile lengths were compared with the actual pile length as found in the As-built drawing or field excavation by TxDOT. TxDOT personnel excavated the site location at Mountain Creek on FM 916 to check the depth of the foundation. The other two bridge depth were confirmed by TxDOT from their as built drawing after the investigation program. The comparison of the unknown foundation depth using resistivity imaging with other test method and actual pile length is presented in Table 4.1

Table 4.1 Comparison of Field Investigation Result

Location of Bridge Site	FDN Type	Foundation ID	Field Investigation Method	Unknown Foundation Depth	Actual Depth	Remarks
Chamber Creek on FM 916, Grandview, Texas	Steel H-Pile	P1E, P2E, P3E, P4E	2D RI test	4 ft	4 ft	Successful
		P1W, P2W, P3W	2D RI test	4 ft		
		P4W	2D RI test	Not Successful	4 ft	
Division Street, Arlington, Texas	Drill Shaft	P1, P2, P3, P4, P5	2D RI test	10ft	30 ft	Not Successful
		P1', P2', P3', P4', P5', P6', P7'	3D RI test	10ft		

Table 4.1 - continued

Location of Bridge Site	FDN Type	Foundation ID	Field Investigation Method	Unknown Foundation Depth	Actual Depth	Remarks
Mountain Creek, FM 2738, Fort Worth, Texas.	Steel H-Pile	P1, P2, P3	2D RI test	14.25 ft	14 ft	Successful
		P4	2D RI test	6.5 ft	7 ft	
		P1	Parallel Seismic Test, Casing backfilled with Cement Grout	14.0 ft	14 ft	Successful
		P1	Parallel Seismic Test, Casing backfilled with Sand	14.5 ft		
		P1	Sonic Echo Test	30.5 ft	14 ft	Not Successful

4.3 Discussion on the Field Investigation Program

The RI test method was observed suitable for the determination of unknown foundation depth for the bridge supported by driven steel H-pile. Compared to the actual bridge foundation depth, the 2D RI methods provide reasonable good results for determination of steel H pile foundation depth for the two bridges supported by steel H-pile. The other bridge foundation supported by drill shaft cannot be determined due to its higher penetration depth that the depth covered by RI. The penetration depth during resistivity imaging depends on the spacing of the electrodes, total number of electrodes in a single line, type of array and type of the soil. The penetration depth for 2D and 3D resistivity imaging performed at Bridge site over Division street, Arlington, Texas supported by drill shaft was found around 24 ft and 15 ft respectively. 2D resistivity imaging for the bridge site at Division Street, Arlington, supported by drill shaft was performed along the direction of traffic. Due to limited accessibility, no 2D resistivity imaging was possible across the traffic direction. Therefore the penetration depth cannot be increased. Thus the disturbed zone cannot be detected and test was not successful to determine drill shaft length using both 2D and 3D resistivity imaging. The comparison of penetration depth from RI test with the investigated foundation depth and actual foundation depth is presented in Table 4.2. From Table 4.2, it was observed that the RI test to determined unknown foundation depth was successful when the penetration depth was higher the actual foundation depth.

Table 4.2 Comparison of Penetration depth from RI test with foundation depth

Location of Bridge Site	Field Investigation Method	Measured Foundation Depth	Max. Penetration Depth from RI test	Actual Depth	Remarks
Chamber Creek on FM 916, Grandview, Texas	2D RI test	4 ft	11 ft	4 ft	Successful
	2D RI test	4 ft	11 ft		
Division Street, Arlington, Tx	2D RI test	10ft	24 ft	30 ft	Not Successful
	3D RI test	10ft	16 ft		
Mountain Creek, FM 2738, Fort Worth, Tx.	2D RI test	14.25 ft	22.5 ft	14 ft	Successful
	2D RI test	6.5 ft	22.5 ft	7 ft	

The Parallel Seismic test was performed at one pile location at the bridge at Mountain Creek on FM 2738, Fort Worth, Texas. This test also includes two casing backfilled with cement grout and sand backfill. The investigated depth using PS shows a good agreement with the actual pile length. However, the signal strength observed from PS test using sand backfill casing shows stronger signal strength compared to PS test performed at cement grout backfilled casing.

The Sonic Echo test performed at the same pile where the PS test is done. From the Sonic Echo test, the data signal reflected from the end of the pile foundation was very weak and repeatedly amplified to determine the foundation depth. Thus depth determined from the Sonic Echo test was misleading for this site.

Parallel Seismic and Sonic echo test provides foundation depth for a single pile test. Parallel Seismic test requires a casing installed parallel to the length of the foundation within 10 ft from the foundation. However, Resistivity Imaging is invasive and provides continuous profile from which the information of the group pile can determined from a single test which may makes the test program cost effective.

CHAPTER 5

CONCLUSIONS AND RECOMMENDATIONS

The unknown bridge foundations pose a significant problem to bridge owners because of safety concerns. The current paper presents the determination of unknown bridge foundation depth at three bridge foundations. Two of bridges are supported by driven steel H-pile foundation. The other bridge is supported by Drill Shaft. Resistivity Imaging was performed to determine the foundation depth. During the field investigation program, 2D resistivity imaging was performed at two bridges supported by steel H-pile. On the other hand, both 2D and 3D resistivity imaging was performed for the bridge supported by drill shaft. The intent of this study is to determine the applicability of the resistivity imaging to determine the unknown foundation depth. Beside the resistivity imaging, Parallel Seismic method and Sonic Echo method was utilized for one bridge site to determine the unknown foundation depth.

5.1 Summary and Conclusions

The investigation results can be summarized as:

- 2D resistivity imaging was performed at both east and west side of the bridge at Chamber Creek on FM 916 to determine unknown foundation depth. From the resistivity imaging, a disturbed zone was found from the resistivity which was considered as foundation depth. The foundation depth investigated from RI was 4 ft from the ground surface. The depth of the foundation was confirmed by TxDOT from site excavation.

- 2D and 3D resistivity imaging was performed at the bridge over Division Street, Arlington supported by drill shaft. Both the 2D and 3D RI provides a variation of

resistivity at 3m or 10 ft depth. However the depth of penetration was up to 24 ft from ground surface. Due to limited site access, the length and spacing of the electrodes cannot be increased to increase the penetration depth. The actual pile length of the foundation was 30 ft. Compared to actual foundation depth, the investigation was not successful due to limited site access and penetration depth.

- 2D resistivity was performed at bridge site at Mountain Creek over FM 2738, Fort Worth, Tx. From the site investigation, the top 7 ft of foundation soil is highly plastic clayey soil (USCS Classification: CH). Disintegrated Eagle Ford Shale was found immediately below the clayey soil followed by stiff Eagle Ford Shale. From Resistivity Imaging, a high resistivity zone was observed and the foundation depth was determined as 14.25 ft from that zone which was very close to the actual pile depth. From the resistivity investigation result, a pile foundation with shorter length was also determined which was also confirmed by as built drawing after the investigation. Thus, pile foundation having difference is length can be determined from a single RI test.

- Parallel Seismic and Sonic echo test was also performed at the bridge site over FM 2738. Only one pile was investigated during this study. Two casing pipe were installed beside the foundation backfilled with cement grout and sand. The test results showed that, signal strength for sand backfilled casing was higher compared to the cement grout backfilled casing. The depth determined from the PS test was 14.0 ft for test performed at cement grout backfilled casing and 14.5 ft for test performed at sand backfilled casing. The test results were very close to the actual foundation depth.

- The reflected signal strength from SE test was very weak due to the higher surface area of the H-pile compared to the cross sectional area. The H-pile foundation depth determined from the SE test was 30.5 ft which was not clear and provides a misleading foundation depth comparing to the actual foundation depth.

- Parallel Seismic and Sonic echo test provides foundation depth for a single pile test. Parallel Seismic test requires a casing installed parallel to the length of the foundation within 10 ft from the foundation. However, Resistivity Imaging is invasive and provides continuous profile from which the information of the group pile can determined from a single test which may make the test program cost effective.
- The resistivity imaging provides good indication to determine unknown foundation depth for shallow steel H-pile foundation. However, a Parallel Seismic method is recommended with resistivity method for cross check of the foundation depth. Using both PS and RI together, the foundation depth can be determined.

5.2 Recommendation for Future Studies

To make the current study even more effective, it is recommended that the work is further continued as mentioned in this section:

1. Two bridges with steel H-pile foundation and one bridge supported by drill shaft was investigated during this study. Determination of depth of Drill Shaft using resistivity imaging method was not successful for this current study. Thus more investigation can be performed on different bridge sites supported by drill shaft.
2. Different types of bridge foundation (example: timber piles, concrete bridge abutments, bridges supported by shallow foundation) can be investigated using Resistivity Imaging.
3. The Resistivity imaging can be performed at different soil profile and geologic condition to investigate the unknown foundation depth.
4. The effect of water table was not considered during this study. The variation of the resistivity will affect the resistivity of the soil. Thus the effect of water table can be studied to determine the unknown foundation depth using resistivity imaging.
5. Dipole-Dipole array is utilized during this study. However, the other array configuration can be studied to determine the unknown foundation depth using Resistivity Imaging.

REFERENCES

1. Finno, R. J., Gassman, S. L., and Osborn, P. W. (1997). “Non-Destructive Evaluation of a Deep Foundation Test Section at the Northwestern University National Geotechnical Experimentation Site.” Federal Highway Administration, Washington, D.C., June.
2. Gassman, S. L., and Finno, R. J. (1999). “Impulse Response Evaluation of Foundations using Multiple Geophones.” J. Perf. Constr. Facil, 13 (2), 82-89.
3. Olson, L. D., Jalinoos, F., and Marwan, F. A. (1998), “Determination of Unknown Subsurface Bridge Foundations”, Geotechnical Guideline No. 16, A summary of NCHRP 21-5 Interim report, Federal Highway Administration, Washington, D.C., August .
4. Olson L. D., Aouad M. F., and Sack D. A. (1998)[b], “Nondestructive Diagnosis of Drilled Shaft Foundations.” Transportation Research Record No. 1633, Transportation Research Board, Washington, D.C., 120–127
5. Sack, D. A., and Olson, L. D. (2009), “Combined Parallel Seismic and Cone Penetrometer Testing of Existing Foundation for Foundation Length and Evaluation”, Proc., Int. Found. Equip. Expo., ASCE, Reston, Va., 544-551.
6. Samouëlian, A., Cousin, I., Tabbagh, A., Bruand, A., and Richard, G. (2005), “Electrical Resistivity Survey in Soil Science: A Review.” Soil & Tillage Research, 83 (2), 173-193.
7. Mercado, E. J., and O'Neill, M. W. (2000), "Geophysical survey techniques to determine lengths of piles and drilled shafts." Proc., Geo-Denver 2000, ASCE, Reston, Va., doi:10.1061/40521(296)10.

8. Stegman, B. G., and Holt, J. D. (2000), "Determining the Capacity of Unknown Foundations." Proc., GeoDenver 2000, ASCE, Reston, Va., doi: 10.1061/40521(296)10.
9. Yu, X. B., Fang, J., Zhang, B., Adams, J., and Lin, G. (2007), "Unknown Foundation Testing: A Case Comparison of Different Geophysical Methods." Proc., 7th Int. Symp. on Field Measurements in Geomechanics, ASCE, Reston, Va., doi:10.1061/40940(307)6.
10. Robinson, B., and Webster, S., (2008), Successful Testing Methods for Unknown Bridge Foundations. Proc. of Fifth Highway Geophysics - NDE Conference: Charlotte, NC; 101-110.
11. Huang, D. Z., and Chen, L. Z. (2007), “3-D Finite Element Analysis of Parallel Seismic Testing for Integrity Evaluation of In-Service Piles”, Proc. Geodenver 2007, ASCE, Reston, Va., doi:10.1061/40908(227)10
12. Olsen, P. A., Binley, A., Henry-Poulter, S., and Tych, W. (1999), “Characterizing solute transport in undisturbed soil cores using electrical and X-ray tomographic methods”. Hydrol. Process. 13, 211–221.
13. Tabbagh, A., Dabas, M., Hesse, A., and Panissod, C. (2000), "Soil resistivity: a non-invasive tool to map soil structure horizonation." Geoderma, 97(3-4), 393-404.
14. Briaud, J. L., Ballouz, M., and Nasr, G. (2002). "Defect and Length Predictions by NDT Methods for Nine Bored Piles." Proc., Int. Deep Foundations Congress 2002, ASCE, Reston, Va., doi: 10.1061/40601(256)13.
15. Maganti, D. (2009). Subsurface Investigations using High Resolution Resistivity, MS Thesis, UT Arlington, Arlington, TX .
16. Hubbard, J. L. (2010). "Use Of Electrical Resistivity And Multichannel Analysis Of Surface Wave Geophysical Tomography In Geotechnical Site Characterization Of Dam." MS Thesis, UT Arlington, Arlington, TX .
17. Telford, W. M., Geldart, L., and Sheriff, R. E. (1990), “Applied geophysics”. Second Edition: Cambridge Univ Pr.

18. Kearey, P., Brooks, M., and Hill, I. (2002). An introduction to geophysical exploration. Wiley-Blackwell, .
19. Banton, O., Seguin, M. K., and Cimon, M. A. (1997). "Mapping field-scale physical properties of soil with electrical resistivity." Soil Sci.Soc.Am.J., 61(4), 1010-1017.
20. Loke, M. (1999). "Electrical imaging surveys for environmental and engineering studies." A Practical Guide to, .
21. Advanced Geosciences, Inc. (2006)."Instruction Manual for EarthImager 2D Version 1.7.4. Resistivity and IP Inversion Software." P.O. Box 201087, Austin, Texas 78720. Tel. (512) 335-3338, Fax (512) 258-9958, www.agiusa.com.
22. Wikimedia Foundation. Inc (2011). "Geology of the Dallas–Fort Worth Metroplex." <http://en.wikipedia.org/wiki/Geology_of_the_Dallas%E2%80%93Fort_Worth_Metroplex> (May 30, 2011).
23. Hall L. L, (2011)[a], "Geology of Tarrant County, Texas" <http://northtexasfossils.com/geologytarrant.htm>(June 20,2011)
24. Hall L. L, (2011)[b], "Johnson County, Texas" <http://northtexasfossils.com/geologyjohnson.htm>(June 20,2011)
25. The Walter Geology Library (2010),"Geology of Texas" <http://www.lib.utexas.edu/geo/pics/texas92a.jpg> (May 28, 2011)
26. USDOT (2009)," Resistivity Methods", <http://www.cflhd.gov/resources/agm/geoApplications/SurfaceMethods/933ResistivityMethods.cfm>(May 28, 2011)

BIOGRAPHICAL INFORMATION

Mohammad Sadik Khan graduated with a Bachelor of Science in Civil Engineering from Bangladesh University of Engineering and Technology, Dhaka, Bangladesh in June 2007. After graduation, he started his career as Assistant Engineer in China National Electric Wire & Cable Import/Export Corporation (CCC). On December 2007, he joined Sinamm Engineering Limited, Dhaka, Bangladesh as Assistant manager and served as a Project Coordinator from April 2009 to December 2009. He started his graduate studies at The University of Texas at Arlington in Spring 2010. During his study, he got the opportunity to work as a graduate research assistant under supervision of Dr. Sahadat Hossain. The author's research interests include determination o f Unknown Foundation using NDT method, Slope stability analysis, Numerical modeling, Analysis and design of Deep foundation, Retaining wall, Excavation support system and Bioreactor Landfills.